A CONTINUUM MECHANICS MODEL OF STRESS MEDIATED ARTERIAL GROWTH DURING HYPERTENSION USING AN EULERIAN FRAME

A Dissertation

by

MAYA ELISE JOHNSON

Submitted to the Office of Graduate and Professional Studies of
Texas A&M University
in partial fulfillment of the requirements for the degree of

DOCTOR OF PHILOSOPHY

Chair of Committee,	Jay R. Walton
Committee Members,	Kumbakonam Rajagopal
	Francis Narcowich
	Peter Howard
Head of Department,	Emil Straube

August 2015

Major Subject: Mathematics

ABSTRACT

Hypertension is a medical condition in which persistent high blood pressure causes the heart to exert more energy to circulate blood through the blood vessels and can lead to life threatening conditions including stroke, heart attack and atherosclerosis. Previous attempts to model arterial growth due to hypertension have made use of kinematic growth and mixture theory models to introduce a continuum mechanics approach to the problem. In this dissertation, we are concerned with modeling arterial growth due to hypertension using a non traditional continuum mechanics approach motivated by the belief that the arterial growth taking place during hypertension is best studied in an Eulerian frame due to its ever-changing nature where one has no a priori knowledge of a "reference" state.

This study has a two-fold purpose: First, illustrate how one can formulate nonlinear elasticity in the "current configuration" and, second, apply that framework to both an isotropic constitutive relation and an anisotropic Holzapfel-Ogden constitutive relation in order to model the biologically dynamic process of stress-mediated growth that occurs during hypertension. We conclude that using an Eulerian framework allows us to solve the nonlinear elasticity problem associated with growth without needing to keep track of evolving reference configurations, with the trade-off being that the formulas are more complex. Using this framework, we test the performance of two popular competing assumptions for the increase in the rate of mass production as a function of stress; namely, a continuous growth criterion and a bang-bang method.

The present model for growth during hypertension assumes that growth results from a perturbation of the arterial wall stress away from homeostasis. In particular, this means that growth only occurs at points through the thickness of the wall where the stress exceeds homeostasis. It has been conjectured that such growth occurs to drive the stress back to

this homeostatic stress state. The results of this dissertation give insight that suggests it is possible for the growth process to return the wall stress back to homeostasis using both the continuous criterion and the bang-bang method for growth, although the bang-bang method does so in less time.

DEDICATION

To my loving mother, Veronica Johnson, who always believed I could do anything.

ACKNOWLEDGEMENTS

I will begin by thanking the person with whom I have worked most closely during this most recent leg of my academic career at Texas A&M - my adviser, Dr. Jay Walton - for all of his tireless support, sincere encouragement and unfailing wisdom. He not only provided me the tools to build the necessary skills I have through his patient and directed tutelage, but he instilled in me a love for Mathematical Biology. Because of Dr. Waltons persistence I now find that whenever Im reading any literature in the field I have to stop and critically ask of myself, “Do I buy into this or that?”, Is there another way of approaching a problem than presented?, or Is there a different way of looking at something altogether?. I would also like to thank my other committee members; Dr. Francis Narcowich, for being the kind of teacher to encourage small bites to consume large concepts; Dr. Kumbakonam Rajagopal, for his unyielding great expectations; and Dr. Peter Howard, for sharing his expertise. I thank them all for their encouragement and support through the arduous tasks of paper writing and presentations.

I turn secondly to my academic roots at Lincoln University in Pennsylvania. Although I would later need to take a few extra classes starting off at Texas A & M, due to the somewhat limited math courses available at the smaller Lincoln University campus, I received an incredibly solid fundamental mathematical core given to me by the highly dedicated and immensely capable teachers at Lincoln University. I would like to especially thank Dr. Guru Nagase, one of the most devoted and exceptional teachers I have ever had. In truth, he was so devoted to me and my future that he was more like a father and still calls to this day to ask if I am most importantly enjoying Math.

I will end with what is more accurately my beginnings. I thank my family. Thank you to those who gave me life, who have been the primary source of support and who

have been and continue to be my biggest fans my whole life - my parents, Charles and Veronica Johnson. Thank you to those who always provided encouragement and a second place to call home throughout my graduate career and in life - my Godparents, Roswell and Alenda Johnson. Thank you to my siblings, especially my sisters, who are my best friends, and who have always been there for me when I needed them. Thank you to my fellow graduate students who over the years have become a very special kind of family. Thank you all, because no one who achieves success does so without the help of others.

TABLE OF CONTENTS

Page

LIST OF FIGURES

FIGURE Page

1. INTRODUCTION

1.1 Background

Hypertension is characterized by chronic high arterial blood pressure with a reading of 140/90mmHg or higher being considered hypertensive. The reason for choosing to study hypertension is that, in addition to being one of the more fundamental, chronic and prevalent arterial diseases to study, it has a strong correlation with other life threatening cardiovascular diseases like atherosclerosis and can lead to a stroke or a heart attack. Therefore, gaining some valuable knowledge of hypertension could have a mitigating effect on those other conditions, which combined are the number one killer in the western world.

Using a continuum mechanics approach to model biological diseases has a long history in the mechanobiology literature. Mechanobiology refers to a biological response to mechanical stimuli. The idea that mechanical forces can invoke biological responses is one that has been proven by a number of experts in the field starting with the work done by Rosen et al in 1974. They showed that endothelial cells experience a 3.7 fold increase in the rate at which they produce histidine decarboxylase, which is an essential enzyme to the synthesis of histamine, when subjected to altered mean shear stress [64]. Histamine is an effector of vascular permeability and is a vasodilator. Further examples of mechanobiology includes the work done by Leung et al wherein they cultured vascular smooth muscle cells on sheets of elastin and subjected them to cyclic uniaxial stretching which increased the production of extracellular matrix proteins 3 to 5 fold [46]. Also, of particular relevance to the current work, Matsumoto and Hayashi reported that sustained high blood pressure during hypertension causes the wall of the artery to thicken or grow [52]. Because of the major role that mechanobiology plays in arterial diseases like hypertension, developing models to understand the mechanical behavior of arteries is a step

towards a better understanding of disease progression and treatment [51].

1.1.1 Continuum Mechanics Models for Growth

Richard Skalak was one of the first to introduce a continuum mechanics approach to the study of growth in the 1980s. He developed the concept of "kinematic growth" which assumes that growth can be modeled through kinematic deformation [65, 66]. This idea was later extended by Rodriguez et al to include incompatible growth [62]. One of the key ideas of "kinematic growth" is that there exists a deformation gradient, $\mathbf{F}_1 = \mathbf{F}_e\mathbf{F}_g$, which is the product of a growth deformation gradient, $\mathbf{F}_g$, and an elastic deformation gradient, $\mathbf{F}_e$, where the elastic part is there to "smooth" out any incompatibilities in the growth process. Finally, the total deformation gradient is then thought of as $\mathbf{F} = \mathbf{F}_2\mathbf{F}_1$ where $\mathbf{F}_2$ is just the classic deformation gradient that takes the body from an unloaded to a loaded configuration. Many others have utilized this "multiplicative" growth formulation to model certain aspects of growth including arterial adaptation to changes in flow rate and pressure [68, 69, 58, 20, 71, 50, 25, 29, 43, 3].

Among the studies listed above is the work by Larry Taber. He was one of the first to address using a continuum mechanics approach for the study of mechanobiology, that is, biological growth (change in mass) and remodeling (change in structure) resulting from a mechanical stimulus [37, 68]. In particular, he extended the idea of Skalak's volumetric growth to model certain aspects of the mechanobiology of growth and remodeling. After his 1995 review, he wrote papers with Eggers and Humphrey on stress-modulated growth in the aorta where they used growth laws that were dependent on material properties and growth parameters [70, 71]. Before this, others had only used continuum mechanics models for growth without a real consideration of the underlying biological processes.

One concern of those who question the purely kinematic treatment of growth is that due to its dynamic nature, with gains and losses of material over time, the question of whether

a fixed reference configuration still exists becomes unclear [40, 4]. Another concern, particularly with those interested in the mechanobiology of growth processes, is that the pure kinematic consideration of growth excludes an explicit treatment of mass production and mass balance which is what defines biological growth.

In consideration of modeling mechanobiological processes such as growth and remodeling, Humphrey and Rajagopal employed a modified mixture theory along with evolving "natural" configurations which were intended to compensate for the uncertainty of a fixed reference configuration for growth [40]. Their paper was motivated, in part, by Fung's work in which he calls for mass-stress relations [22]. They also used mixture theory to model the ability of arteries to adapt to alterations in blood flow rate [41]. In both papers, they modeled the arterial wall as a mixture of structurally significant constituents including elastin, collagen and smooth muscle cells, where each constituent has mass production and removal rates that are dependent on the arterial wall stresses and strains. Their notion of evolving naturals configurations assumes that each constituent is created in its own stress-free natural configuration from which it gets deposited into the body and is endowed with a preferred deposition stretch. The natural configurations are then allowed to change as the body grows and evolves. Still, the issue of determining reference or natural configurations for growth remains complex. In a review article by Ambrosi et al, it was acknowledged that one major challenge in modeling growth is "identifying reference configurations for growing tissues," they go on further to suggest that one solution to this problem would be to eliminate the use of reference configurations and formulate elasticity in the current configuration, in which case, one would only need to know how residual stressed evolved [2]. Herein lies the motivation behind the current work that illustrates how to formulate nonlinear elasticity in the current configuration and employs it to model how the mechanical stimuli of chronic high blood pressure drives arterial growth and how growth occurs to drive circumferential arterial wall stress back to homeostasis.

1.2 Thesis Outline

Throughout this thesis we keep as a guide Humphrey's five basic steps for constitutive formulations:delineate general characteristic behaviors; establish an appropriate theoretical framework; identify specific functional forms of the requisite relations; calculate values of the associated material parameters, and evaluate the predictive capability of the final relations [37]. To that end, in chapter 2 we start with the first of the five steps by examining the fundamental characteristics of arteries, including their structure and their constitutive make-up. These characteristics also refer to the mechanical properties of arteries, which describe their material response to applied loads. We also discuss their characteristic behaviors as living tissue, in specific, their ability to grow and adapt to changes in their mechanical environment. This adaptive behavior becomes more evident with a more in depth look at mechanobiology in the context of arterial growth and remodeling. An example of arterial growth and remodeling, which is also the focus of this dissertation, is hypertension. Therefore, we take a separate look into some mechanobiological processes present in hypertensive arteries, with a specific focus on appropriate assumptions based on important biological contributors to arterial growth due to hypertension. Although it is undoubtedly not possible to account for every factor in the mechanobiology of hypertension, it is an important task to determine which are fundamentally intrinsic to growth processes occurring as a result of hypertension. Lastly, since we are considering stress modulated arterial growth, we discuss a mass-stress relation which is based on the existence of a homeostatic stress state for the arterial wall.

In chapter 3, we move on to step two of the five by proposing that an appropriate theoretical framework is one that is formulated entirely in the current configuration with a look at what goes in to the formulation of elasticity in an eulerian frame. We have an overall theme of showing how one can move from conventional ideas involving the use

of a reference configuration to ones that only need a working knowledge of the current configuration. This starts with a preliminary discussion of kinematics. Kinematics deals with motions and deformations and it is within the context of kinematics that we define the concept of a reference and a current configuration. This is followed by a treatment of elasticity, which includes a detailed illustration of how the Cauchy stress tensor, $\mathbf{T}$, depends on the gradient of a scalar strain energy function taken with respect to eulerian strain tensors $\mathbf{e}$ and $\mathbf{d}$ for the isotropic and anisotropic case respectively. For the isotropic case, we consider an incompatible neo-hookean constitutive relation to model the strain energy function, while for the anisotropic case we use a Holzapfel-Ogden constitutive relation [34]. For both cases, we use a modified version of the constitutive relation, that is, one formulated in the current configuration. We then use a Fung-type multiplicative incorporation of residual stress posed by Gorb and Walton [28]. For both the isotropic and anisotropic cases we assume a simplified tubular geometry for the artery and, imposing axisymmetry and making use of a semi-inverse approach, calculate the desired wall stresses.

At this point in the thesis we will have considered steps one and two of Humphrey's five steps for constitutive formulations, namely, delineating general characteristic behaviors and establishing an appropriate theoretical framework. Although not explicitly mentioned, we also identified functional forms, which is step three, for the strain energy function by adopting the isotropic and anisotropic constitutive relations. Furthermore, although actually calculating material parameters often involves some manner of curve-fitting which is outside the scope of this dissertation, we have incorporated the fourth step by utilizing previously calculated material parameters in our model. In chapter 4 we continue to employ steps three and four as we describe our model for stress mediated growth, and in particular, our mass-stress growth law. We first look at some previous treatment of stress modulated growth due to an increase in arterial pressure with specific attention to growth laws and mass-stress relations. Next, we look at our model where we incorporate assump-

tions discussed in chapter 2 about the mechanobiology of hypertension to define how the mass production rate depends on wall stress. In addition, assumptions we made about the key contributors to arterial growth during hypertension go into the growth model as well in the form of material parameters, in the case of smooth muscle turnover rates. We also look at two different models for how growth is initiated and at what rate material is added to the arterial wall. The first method, herein referred to as the continuous method, assumes that the rate at which mass is being added is a continuous function of a radially dependent stress measure. So that for some initial starting time, when growth processes are activated, material is added at a maximum rate and then mass production decreases from that maximum rate, eventually reaching a leveling off point. In contrast, the second method, herein referred to as the bang-bang method as it is most commonly known in control theory, assumes that mass is added at a constant and maximum rate.

Finally, in chapter 5 we discuss what Humphrey appropriately considers to be one of the most important steps in the five-step process, and that is step five: Evaluate the predictive capability of the final relations. In the results section we test both the isotropic and the anisotropic models using the competing continuous and bang-bang methods. In the isotropic case we compare the performance of the continuous and bang-bang methods, in particular, we test the ability of each to predict the thickening of the arterial wall and to return the circumferential wall stress back to homeostatic levels. Making the same comparison for the anisotropic case revealed that both the continuous and the bang-bang methods performed better than they had in the isotropic case, meaning it took considerably less time for the circumferential arterial wall stress to return to homeostasis. This is to be expected since arteries are inherently anisotropic and so an anisotropic model is more appropriate. In the last chapter we give some discussion including possible improvements to the current model and future work.

2. MECHANOBIOLOGY AND HYPERTENSION

2.1 Structure of the Arterial Wall

Arteries have a tubular-like geometry, often modeled as an idealized tube, in which the lumen is the opening in the center where the blood flows through the artery. In general, there are two main types of arteries: elastic and muscular. Elastic arteries, like the aorta and main pulmonary artery, are usually larger in diameter and are closer to the heart; whereas muscular arteries, like the coronaries and the cerebrals, are smaller in diameter and are located closer to the arterioles. Regardless of type, location or function, all arteries consist of three layers: the intima, the media, and the adventitia. Depending on arterial function, the thickness of each layer may differ from artery to artery. The intima is the innermost layer and consists of a single layer of endothelial cells and a thin basal lamina that separates it from the blood flowing through the lumen. Some elastic arteries have a subendothelial layer that contains connective tissue and smooth muscle cells. The media is the middle layer and contains primarily smooth muscle cells embedded in an extracellular network of collagen, elastin, and proteoglycans. Smooth muscle cells are oriented circumferentially in most arteries [61] and make up 25% to 60% of the arterial wall [53]. The third layer is called the adventitia and is the outermost layer. The adventitia is mostly comprised of type I collagen, fibroblasts, and the vaso vasorum. The adventitia is thought to mitigate acute over-extension of vessels [35]. It is assumed that the medial and adventitial layers are structurally most important. Furthermore, the adventitia makes up less than 10% of the arterial wall in elastic arteries [35]. In our study, therefore, we exclude the intimal and adventitial layers for a simplified one layer model of the artery.

2.2 Mechanical Properties of Arteries

When developing a stress-driven growth model it is important to start with a proper model of arterial wall stress that incorporates salient mechanical properties of the arterial wall. Soft tissues such as arteries undergo large finite deformations and are hyperelastic [35], anisotropic and heterogeneous [34, 26, 18, 12, 35] with anisotropy mostly due to different orientation of collagen fiber families, are nearly incompressible, and are residually stressed [8, 10, 11, 12, 24, 48, 49]. The fact that arteries undergo large deformations cannot be overlooked. Models more suited for materials that experience small strains would be an over simplification that could not hope to capture actual mechanical behavior of arteries which is essential for modeling mechanobiological processes.

Arteries are layered and therefore are heterogeneous. As was discussed in some detail in the previous section, the arterial wall is viewed as consisting of three layers. The three layers are known as the intima which is the innermost layer, the media which is the layer in the middle and the adventitia which is the outermost layer. Within the layers there are three structurally significant constituents known as elastin, collagen (mainly types I, III, and V), and smooth muscle cells. Work done by Clark and Glagov suggested that the constituents were distributed uniformly within each layer. For instance, the distribution of smooth muscle cells in the media only differed in regions on the border of the intimal or the adventitial layers [13]. With this we assume that even though the arterial wall as a whole is heterogeneous, within each layer there is homogeneity. Furthermore, as mentioned above, we go on to assume that when modeling growth processes we can ignore the intimal layer. We also exclude the adventitial layer from our model. Such an assumption is mostly reasonable for elastic arteries where the adventitia makes up less than 10% of the arterial wall. Furthermore, it is thought that the media is the main effector of mechanobiological processes [37]. This is not to say that the intimal and the adventitial layers do not play

an important part in growth and remodeling of the arterial wall during hypertension. For instance, smooth muscle cells in the media receive vital nutrients via diffusion through the intima, and, in thicker arteries, through the vaso vasorum located in the adventitia. Also, both the intimal and the adventitial layers provide the arterial wall with some structural support.

Finally, another property of arteries that is important and needs to be treated carefully is the observation that they are residually stressed. Residual stress is defined as the stress that is present in the body in the absence of applied loads and is usually a result of internal biological processes. This characteristic of arteries was observed by Y.C. Fung and colleagues. He radially cut an excised cross-sectional slice of an artery and observed that the artery sprang open suggesting that it was under some internal stress. Residual stress is important mechanically because if residual stress is present that contributes to the difficulty of finding a "stress-free" reference configuration. That is, with the existence of residual stress, the material body is never completely stress-free. The concept of residual stress in the context of mechanobiology is an important one as well. Without the inclusion of residual stress, the intimal circumferential wall stress becomes very high while a residual stress of roughly 3kPa is enough to reduce the stress by hundreds of kPa [21]. Also, Clark and Glagov showed how only when they incorporated residual stress in their model did the circumferential component of the arterial wall stress have a nearly uniform distribution which is what is observed in nature [13]. Furthermore, it is presumed that growth and remodeling processes that take place during development do so to achieve this nearly uniform stress distribution in maturity, and that this is a homeostatic stress state for the arterial wall [37]. Observations support the existence of mechanical homeostasis in biology and pathobiology [36]. Determining residual stresses in the body, however, still continues to be a challenging problem with recent efforts including work done by Joshi and Walton, and Gou and Walton where they used ultrasound techniques and inverse spec-

tral techniques to reconstruct residual stresses for soft tissues[42, 30]. For the purpose of this study, we simply adopt a model for the residual stresses that arise as a consequence of growth and remodeling processes such as ones found in the work done by Humphrey and others [7, 33, 35].

2.3 Mechanobiology

Y. C. Fung commented that while developing theories for the biomechanics of soft tissues, we must remember that they are *living*, able to grow, replicate, and adapt [23]. Motivated by this reminder, Humphrey suggested that employing a biomechanics approach to modeling arteries should not simply consist of applying classical theories in mechanics to arteries but rather should be an extension of the theories with the purpose of capturing constitutive characteristics of living tissue, specifically their ability to adapt due to mechanical changes in their environment [37]. As mechanobiology is the study of how biological tissues respond to mechanical stimulation, not merely through deformation but through growth and adaptation, biomechanics should be an extension of mechanics aimed at answering questions of interest in mechanobiology. We discussed some evidence of the mechano-sensitivity of cells, however, there are still many more examples [14, 9, 31, 45, 47]. Romer et al show that focal adhesions can be targets for mechanical stimuli that evoke biological processes such as cell growth [63]. Williams focuses on the direct effects that arterial wall stress has on vascular smooth muscle cells. He asserts that wall stress strongly influences the orientation, growth and phenotype of cultured vascular smooth muscle cells [74]. Fridez et al claimed that smooth muscle tone was also affected by mechanical stimuli. That is, smooth muscle contractility is also sensitive to changes in arterial pressure [20].

An area of mechanobiology of particular importance in the study of cardiovascular disease is known as growth and remodeling which refer to a change in mass and structure

respectively. In particular, grow and remodeling are processes that are ever present in the body through regular tissue maintenance, that is, the continual production and removal of cells and extracellular matrix [40]. In this context, growth only occurs if there is a net increase in mass, so that material is being added at a faster rate than it is being removed. Other examples of growth and remodeling include early development, aging, wound healing, development of aneurysms, and atherosclerosis. There has been a myriad of work done on such growth and remodeling processes, including the development of appropriate growth and remodeling frameworks [44, 27, 23, 68, 40, 1, 3, 17, 37, 73, 6, 2, 5, 19, 39]. Another example of a disease in which growth and remodeling plays a major role, which is the main focus of this work, is hypertension. A brief discussion on the mechanobiological processes that take place during hypertension is given below.

2.4 Mechanobiology of Hypertension

The mechanobiology of hypertension was briefly mentioned in the previous chapter but more specifically, sustained high blood pressure, which is characteristic of hypertension causes a thickening of the medial layer of the arterial wall [35]. It is clear that changes due to hypertension involve extracellular matrix and smooth muscle cells. Willams too suggests that vascular smooth muscle cells in the media experiences most of chronic wall stress, and also that wall stress increases the ability of vascular smooth muscle cells to release certain growth factors which then influence vascular smooth muscle and endothelial cell growth and function [74]. Smooth muscle cells can either increase in cell size (hypertrophy) or in cell number (hyerplasia) during hypertension, although there are conflicting views and experimental data on whether smooth muscle hypertrophy or hyperplasia takes precedence during hypertensive growth [54, 57, 56].

It is not entirely clear whether growth and remodeling, and in particular growth due to hypertension, is excited by altered stress or altered strain but it has been conjectured to

occur in order to drive the circumferential wall stress back to a preferred or homeostatic value [75]. This seems like a reasonable assumption when one considers that the idea of a target stress value gets repeated throughout the study of growth and remodeling [37]. Keeping with this assumption, we model arterial growth during hypertension as a function of how much circumferential wall stress deviates from this homeostatic target. We do, however, deviate from the popular use of a constant target value, such as the mean wall stress, in favor of a spatially non-homogeneous target. Again, it is unclear whether it is sufficient for the average circumferential wall stress to return to homeostasis or if the body seeks to relieve the stress felt at each point throughout the thickness of the wall. We assume the latter is the case and model stress-mediated growth as a function of the difference between the homeostatic circumferential stress distribution and the hypertensive stress distribution as a function of radial position in the arterial wall. This matter will be address in more detail in chapter 4.

3. ELASTICITY IN THE CURRENT CONFIGURATION

In the classic theory of elasticity, people make use of a fixed reference configuration for the ease of calculating stresses and strains. If this reference configuration is stress-free, we call it a natural configuration. If the reference configuration is "pre-stressed" then there are some boundary tractions present, such is the case for the configuration of a pressurized artery in vivo. Finally, if the reference configuration is residually stressed then there are internal forces present in the absence of boundary tractions which, in the case of soft tissues, may arise from biological growth and adaptation. In Fung's reference of residual stress he considers an intermediate configuration that is residually stressed but traction free and comes from a fictitious natural configuration that is the "cut-ring" configuration. In this work we use the current configuration as our reference because growth occurs in the current configuration and thus there is a compelling argument for formulating elasticity in the current configuration.

For illustrative purposes, in this section we present a formulation of elasticity in the current configuration by first starting from classic theories of continuum mechanics that make use of a fixed reference configuration. We begin with kinematics and notational conventions.

3.1 Kinematics

Kinematics refers to how a material body moves and deforms. Consider the deformation $\boldsymbol{\chi}: \ \mathcal{B}_0 \longrightarrow \mathcal{B}_t$ that describes how points from the reference configuration, $\mathcal{B}_0$, move to points in the current configuration, $\mathcal{B}_t$, so that $\boldsymbol{x} = \boldsymbol{\chi}(\boldsymbol{X}, t)$. Here, $\boldsymbol{x}$ and $\boldsymbol{X}$ represent points in the current and reference configuration respectively. The deformation gradient is defined as $\boldsymbol{F} := \partial \boldsymbol{x}/\partial \boldsymbol{X}$ and the displacement is given by $\boldsymbol{u} = \boldsymbol{x} - \boldsymbol{X}$. Note that both the deformation gradient and the displacement depend on the knowledge of points,

$\boldsymbol{X}$, in the reference configuration. The mapping $\boldsymbol{\chi}$ is continuous and invertible so that $\boldsymbol{X} = \boldsymbol{\chi}^{-1}(\boldsymbol{x}, t)$. Using this observation, one can define the displacement with respect to the current configuration as,

$$\tilde{\boldsymbol{u}} := \boldsymbol{x} - \chi^{-1}(\boldsymbol{x}, t). \tag{3.1}$$

It is important to note that one need only think of χ^{-1} as a function of points in the current configuration, it is not necessary to know χ explicitly just that it exists as a continuous invertible map from the reference to the current configuration. Therefore, in the semi-inverse approach, discussed later, we can propose a functional form for $\tilde{\boldsymbol{u}}$ directly without any knowledge of $\boldsymbol{u}$ and thus without any knowledge of a reference configuration.

The deformation gradient $\mathbf{F}$ is viewed as a material field and so is defined on the reference configuration. The spatial description of the deformation gradient is given as

$$\boldsymbol{F} = (\mathbf{I} - \textbf{grad } \tilde{\mathbf{u}})^{-1}. \tag{3.2}$$

We can then define a spatial strain tensor $\mathbf{d}$ given by

$$\mathbf{d} := \frac{1}{2}(\mathbf{I} - \mathbf{C}^{-1}). \tag{3.3}$$

In (3.3), $\mathbf{C}$ is the Right Cauchy-Green tensor defined as $\mathbf{C} := \mathbf{F}^{\mathrm{T}}\mathbf{F}$, and so $\mathbf{C}^{-1} := \mathbf{F}^{-\mathbf{1}}\mathbf{F}^{-\mathrm{T}}$. The strain tensor $\mathbf{d}$ is the anisotropic analog to the Almansi-Hamel strain tensor given by

$$\mathbf{e} := \frac{1}{2}(\mathbf{I} - \mathbf{B}^{-1}), \tag{3.4}$$

where $\mathbf{B}$ is the Left Cauchy-Green tensor defined as $\mathbf{B} := \mathbf{F}\mathbf{F}^{\mathrm{T}}$, and so $\mathbf{B}^{-1} := \mathbf{F}^{-\mathrm{T}}\mathbf{F}^{-\mathbf{1}}$.

3.2 Elasticity

Elasticity refers to the behavior of a material that has been subjected to applied loads. Arteries are hyperelastic, which means they are non dissipative. Mathematically it means

that the associated 1st Piola-Kirchhoff stress tensor, $\hat{\mathbf{S}}$ can be written as the gradient of a scalar function, $\hat{W}$. In particular,

$$\hat{\mathbf{S}} = \partial_F \hat{W}. \tag{3.5}$$

To formulate elasticity in the current configuration we need to first determine how $\partial_F W(\mathbf{e})$ and $\partial_F W(\mathbf{d})$ relate to $\partial_e W(\mathbf{e})$ and $\partial_d W(\mathbf{d})$ respectively, where $\mathbf{e}$ and $\mathbf{d}$ are the spatial strain tensors discussed in section 3.1. We will first see how this is done for $\mathbf{e}$.

Note that $\partial_F W(\mathbf{e})$ is defined implicitly to be the unique second order tensor satisfying

$$\partial_{\mathbf{F}} W(\mathbf{e}) \cdot \mathbf{H} = \mathsf{D}_{\mathbf{F}} W(\mathbf{e})[\mathbf{H}], \quad \forall \mathbf{H} \in \mathfrak{T}^2, \tag{3.6}$$

where $\mathfrak{T}^2$ is the space of second order tensors. If we apply the tensoral equivalent of the chain rule we have

$$\partial_{\mathbf{F}} W(\mathbf{e}) \cdot \mathbf{H} = \mathsf{D}_{\mathbf{F}} W(\mathbf{e})[\mathbf{H}] = \partial_{\mathbf{e}} W(\mathbf{e}) \cdot \mathsf{D}_{\mathbf{F}} \mathbf{e}[\mathbf{H}]. \tag{3.7}$$

At this point it may be useful to recall some derivatives from tensor calculus. Let $\phi : \mathfrak{T}^2 \longrightarrow \mathfrak{T}^2$ be a tensoral valued function. If $\phi(\mathbf{A}) = \mathbf{A}^{-1}$, then

$$\mathsf{D}_{\mathbf{A}} \psi(\mathbf{A})[\mathbf{H}] = -\mathbf{A}^{-1}\mathbf{H}\mathbf{A}^{-1} \tag{3.8}$$

Moreover, if $\phi(\mathbf{A}) = \mathbf{A}\mathbf{A}^{\mathrm{T}}$, then

$$\mathsf{D}_{\mathbf{A}} \psi(\mathbf{A})[\mathbf{H}] = \mathbf{H}\mathbf{A}^{\mathrm{T}} + \mathbf{A}\mathbf{H}^{\mathrm{T}}, \tag{3.9}$$

and if $\phi(\mathbf{A}) = \mathbf{A}^{\mathrm{T}}\mathbf{A}$, then

$$\mathsf{D}_{\mathbf{A}} \psi(\mathbf{A})[\mathbf{H}] = \mathbf{A}^{\mathrm{T}}\mathbf{H} + \mathbf{H}^{\mathrm{T}}\mathbf{A}. \tag{3.10}$$

Making use of both (3.8) and (3.9) we have that

$$\mathsf{D}_{\mathbf{F}}\mathbf{e}[\mathbf{H}] = -\frac{1}{2}\mathsf{D}_{\mathbf{F}}\mathbf{B}^{-1}[\mathbf{H}] = \frac{1}{2}\mathbf{B}^{-1}[\mathbf{H}\mathbf{F}^{\mathrm{T}} + \mathbf{F}\mathbf{H}^{\mathrm{T}}]\mathbf{B}^{-1}. \tag{3.11}$$

Substituting (3.11) into (3.7) implies

$$\begin{aligned}\partial_{\mathbf{F}}W(\mathbf{e})\cdot\mathbf{H} &= \frac{1}{2}\partial_{\mathbf{e}}W(\mathbf{e})\cdot\mathbf{B}^{-1}[\mathbf{H}\mathbf{F}^{\mathrm{T}} + \mathbf{F}\mathbf{H}^{\mathrm{T}}]\mathbf{B}^{-1} \\ &= \frac{1}{2}\mathbf{B}^{-1}\partial_{\mathbf{e}}W(\mathbf{e})\mathbf{B}^{-1}\cdot[\mathbf{H}\mathbf{F}^{\mathrm{T}} + \mathbf{F}\mathbf{H}^{\mathrm{T}}] \\ &= \mathbf{B}^{-1}\partial_{\mathbf{e}}W(\mathbf{e})\mathbf{B}^{-1}\mathbf{F}\cdot\mathbf{H}.\end{aligned} \tag{3.12}$$

Note that the last step in (3.12) is possible since the tensor $\mathbf{B}^{-1}\partial_{\mathbf{e}}W(\mathbf{e})\mathbf{B}^{-1}$ is symmetric. Therefore, (3.12) implies that

$$\partial_{\mathbf{F}}W(\mathbf{e}) = \mathbf{B}^{-1}\partial_{\mathbf{e}}W(\mathbf{e})\mathbf{B}^{-1}\mathbf{F}, \tag{3.13}$$

and, in particular, (3.5) and (3.13) imply that

$$\hat{\mathbf{S}}(\mathbf{F}) = \mathbf{B}^{-1}\partial_{\mathbf{e}}W(\mathbf{e})\mathbf{B}^{-1}\mathbf{F}. \tag{3.14}$$

From (3.14) and the 1st-Piola-Kirchhoff transform it follows that

$$\begin{aligned}\mathbf{B}^{-1}\partial_{\mathbf{e}}W(\mathbf{e})\mathbf{B}^{-1} &= \hat{\mathbf{S}}(\mathbf{F})\mathbf{F}^{-1} \\ &= \hat{\mathbf{T}}\mathbf{F}^{-\mathrm{T}}\mathbf{F}^{-1} \\ &= \hat{\mathbf{T}}\mathbf{B}^{-1}.\end{aligned} \tag{3.15}$$

Finally, (3.15) implies that

$$\hat{\mathbf{T}} = \mathbf{B}^{-\mathbf{1}}\partial_{\mathbf{e}}W(\mathbf{e}) = (\mathbf{I} - 2\mathbf{e})\partial_{\mathbf{e}}W(\mathbf{e}). \tag{3.16}$$

We now look at the formulation for the spatial tensor $\mathbf{d}$. As before, note that $\partial_F W(\mathbf{d})$ is defined implicitly to be the unique second order tensor satisfying

$$\partial_{\mathbf{F}}W(\mathbf{d}) \cdot \mathbf{H} = \mathsf{D}_{\mathbf{F}}W(\mathbf{d})[\mathbf{H}], \quad \forall \mathbf{H} \in \mathfrak{T}^2, \tag{3.17}$$

If we apply the tensoral equivalent of the chain rule we have

$$\partial_{\mathbf{F}}W(\mathbf{d}) \cdot \mathbf{H} = \mathsf{D}_{\mathbf{F}}W(\mathbf{d})[\mathbf{H}] = \partial_{\mathbf{d}}W(\mathbf{d}) \cdot \mathsf{D}_{\mathbf{F}}\mathbf{d}[\mathbf{H}]. \tag{3.18}$$

Making use once more of (3.8) together with (3.10) we have that

$$\mathsf{D}_{\mathbf{F}}\mathbf{d}[\mathbf{H}] = -\frac{1}{2}\mathsf{D}_{\mathbf{F}}\mathbf{C}^{-\mathbf{1}}[\mathbf{H}] = \frac{1}{2}\mathbf{C}^{-\mathbf{1}}[\mathbf{F}^{\mathrm{T}}\mathbf{H} + \mathbf{H}^{\mathrm{T}}\mathbf{F}]\mathbf{C}^{-\mathbf{1}}. \tag{3.19}$$

Substituting (3.19) into (3.18) implies

$$\begin{aligned}
\partial_{\mathbf{F}}W(\mathbf{d}) \cdot \mathbf{H} &= \frac{1}{2}\partial_{\mathbf{d}}W(\mathbf{d}) \cdot \mathbf{C}^{-\mathbf{1}}[\mathbf{F}^{\mathrm{T}}\mathbf{H} + \mathbf{H}^{\mathrm{T}}\mathbf{F}]\mathbf{C}^{-\mathbf{1}}. \\
&= \frac{1}{2}\mathbf{C}^{-\mathbf{1}}\partial_{\mathbf{d}}W(\mathbf{d})\mathbf{C}^{-\mathbf{1}} \cdot [\mathbf{F}^{\mathrm{T}}\mathbf{H} + \mathbf{H}^{\mathrm{T}}\mathbf{F}] \\
&= \mathbf{F}\mathbf{C}^{-\mathbf{1}}\partial_{\mathbf{d}}W(\mathbf{d})\mathbf{C}^{-\mathbf{1}} \cdot \mathbf{H}.
\end{aligned} \tag{3.20}$$

Therefore, (3.20) and (3.17) imply that

$$\partial_{\mathbf{F}}W(\mathbf{d}) = \mathbf{F}\mathbf{C}^{-\mathbf{1}}\partial_{\mathbf{d}}W(\mathbf{d})\mathbf{C}^{-\mathbf{1}}, \tag{3.21}$$

and, in particular, (3.5) and (3.21) imply that

$$\hat{\mathbf{S}}(\mathbf{F}) = \mathbf{F}\mathbf{C}^{-\mathbf{1}}\partial_{\mathbf{d}}W(\mathbf{d})\mathbf{C}^{-\mathbf{1}}. \tag{3.22}$$

From (3.22) and the 1st-Piola-Kirchhoff transform it follows that

$$\begin{aligned}\mathbf{C}^{-\mathbf{1}}\partial_{\mathbf{d}}W(\mathbf{d})\mathbf{C}^{-\mathbf{1}} &= \mathbf{F}^{-\mathbf{1}}\hat{\mathbf{S}} \\ &= \mathbf{F}^{-\mathbf{1}}\hat{\mathbf{T}}\mathbf{F}^{-\mathrm{T}}\end{aligned} \tag{3.23}$$

Finally, (3.23) implies that

$$\begin{aligned}\hat{\mathbf{T}} &= \mathbf{F}\mathbf{C}^{-\mathbf{1}}\partial_{\mathbf{d}}W(\mathbf{d})\mathbf{C}^{-\mathbf{1}}\mathbf{F}^{\mathrm{T}} \\ &= \mathbf{F}^{-\mathrm{T}}\partial_{\mathbf{d}}W(\mathbf{d})\mathbf{F}^{-\mathbf{1}} \\ &= (\mathbf{I} - \textbf{grad }\tilde{\mathbf{u}})^{\mathrm{T}}\partial_{\mathbf{d}}W(\mathbf{d})(\mathbf{I} - \textbf{grad }\tilde{\mathbf{u}}).\end{aligned} \tag{3.24}$$

As mentioned in section 2.2, residual stress is an important concept in mechanobiolgy. A method for incorporating residual stress posed by Walton and Gorb [28] defines

$$W_R(\mathbf{C};\tau) = W_N(\mathbf{F}_R^{\mathrm{T}}\mathbf{C}\mathbf{F}_R), \tag{3.25}$$

where τ represents the residual stress and $\mathbf{F}_R$ is a "virtual" deformation gradient from a natural "stress-free" configuration to an unloaded residually stressed configuration, so that

$$\mathbf{F}_R = \mathbf{T}_N^{-1}(\tau), \tag{3.26}$$

where $\mathbf{T}_N(\cdot)$ is the natural Cauchy response function. Note too that in the absence of residual stress, $W_R(\mathbf{C};0) = W_N(\mathbf{C})$. Using the fact that $\mathbf{C} = \mathbf{I} - 2\mathbf{d}^{-1}$, (3.25) then

becomes

$$W_R((\mathbf{I}-2\mathbf{d}^{-1});\tau) = W_N(\mathbf{F}_R^{\mathrm{T}}(\mathbf{I}-2\mathbf{d}^{-1})\mathbf{F}_R), \tag{3.27}$$

and (3.24) becomes

$$\mathbf{T}(\mathbf{d}) = (\mathbf{I}-\textbf{grad }\tilde{\mathbf{u}})^{\mathrm{T}}\partial_{\mathbf{d}}W(\mathbf{F}_R^{\mathrm{T}}\mathbf{d}\mathbf{F}_R)(\mathbf{I}-\textbf{grad }\tilde{\mathbf{u}}). \tag{3.28}$$

Note that using $\mathbf{C}$ in the above formulation is convenient since $(\mathbf{F}\mathbf{F}_{\mathbf{R}})^{\mathrm{T}}(\mathbf{F}\mathbf{F}_R) = \mathbf{F}_R^{\mathrm{T}}\mathbf{C}\mathbf{F}_R$, while using $\mathbf{B}$ gives $(\mathbf{F}\mathbf{F}_R)(\mathbf{F}\mathbf{F}_{\mathbf{R}})^{\mathrm{T}} = \mathbf{F}\mathbf{B}_R\mathbf{F}^{\mathrm{T}}$. However, when we impose axisymmetry in the later sections we will see that we have diagonal deformation gradients and so $\mathbf{C}$ and $\mathbf{B}$ will be interchangeable.

Although we would like to be able to determine residual stresses in vivo, doing so has proven to be a very arduous task. Adding to the difficulty is the fact that it is very hard to conduct nondestructive experiments to determine residual stresses. As a consequence of this, we provide in this work an illustration of hypertensive growth using a Fung-like residual stress model for $\mathbf{F}_{\mathbf{R}}$. This paradigm assumes that the stress relieving radial cut relaxes the artery to a stress-free natural configuration. In actuality this process is just an approximation, one would need to make infinitely many cuts to relieve all the residual stress. So $\mathbf{F}_{\mathbf{R}}$ is the deformation gradient associated with a deformation from the "cut-ring" configuration to the unloaded "intact" residually stressed intermediate configuration.

3.3 Using an Isotropic Constitutive Relation

In this section we apply the stress-strain relation determined in section 3.2 to an Incompressible Neo-Hookean constitutive form for the strain energy function W. In particular,

$$W = \frac{\mu}{2}\mathrm{tr}\mathbf{B}. \tag{3.29}$$

Recall that the Almansi-Hamel strain tensor is given by equation 3.4, namely, $\mathbf{e} = \frac{1}{2}(\mathbf{I} - \mathbf{B}^{-1})$. Solving for $\mathbf{B}$ in terms of $\mathbf{e}$ gives

$$\mathbf{B} = (\mathbf{I} - 2\mathbf{e})^{-1} \tag{3.30}$$

If we substitute (3.30) into (3.29), then we get

$$W(\mathbf{e}) = \frac{\mu}{2}\text{tr}(\mathbf{I} - 2\mathbf{e})^{-1}, \tag{3.31}$$

where we take $\mu = 27$kPa [28].

We now need to find the gradient of the scalar strain energy function W with respect to the spatial strain tensor $\mathbf{e}$. Recall that the gradient, $\partial_{\mathbf{e}}W(\mathbf{e})$, is defined implicitly as the unique second order tensor satisfying

$$\partial_{\mathbf{e}}W(\mathbf{e}) \cdot \mathbf{H} = \mathsf{D}_{\mathbf{e}}W(\mathbf{e})[\mathbf{H}], \quad \forall \mathbf{H} \in \mathfrak{T}^2. \tag{3.32}$$

Again, before we find the gradient it is useful to recall derivatives from tensor calculus. Let $\phi : \mathfrak{T}^2 \longrightarrow \mathbb{R}$ be a scalar valued function. If $\phi(\mathbf{A}) = \text{tr}\mathbf{A}$, then

$$\mathsf{D}_{\mathbf{A}}\phi(\mathbf{A})[\mathbf{H}] = \text{tr}\mathbf{H}. \tag{3.33}$$

Also, recall from section 3.2 that if $\psi(\mathbf{A}) = \mathbf{A}^{-1}$, then $\mathsf{D}_{\mathbf{A}}\psi(\mathbf{A})[\mathbf{H}] = -\mathbf{A}^{-1}\mathbf{H}\mathbf{A}^{-1}$.

Making use of (3.33) and (3.8) along with the tensoral version of the chain rule we obtain that

$$\mathsf{D}_{\mathbf{e}}W(\mathbf{e})[\mathbf{H}] = \frac{\mu}{2}\text{tr}(-(\mathbf{I} - 2\mathbf{e})^{-1}(-2\mathbf{H})(\mathbf{I} - 2\mathbf{e})^{-1}). \tag{3.34}$$

With some work and making use of the fact that, for $\mathbf{A}$ and $\mathbf{B}$ in $\mathfrak{T}^2$, $\mathbf{A} \cdot \mathbf{B} = \text{tr}(\mathbf{A}^{\text{T}}\mathbf{B})$, (3.34) becomes

$$\mathsf{D}_{\mathbf{e}}W(\mathbf{e})[\mathbf{H}] = \mu(\mathbf{I} - 2\mathbf{e})^{-2} \cdot \mathbf{H} = \partial_{\mathbf{e}}W(\mathbf{e}) \cdot \mathbf{H}. \tag{3.35}$$

Therefore, (3.35) implies we must have that

$$\partial_{\mathbf{e}} W(\mathbf{e}) = \mu(\mathbf{I} - 2\mathbf{e})^{-2}. \tag{3.36}$$

Recall from section 3.2 that the Cauchy stress, $\mathbf{T}$, is related to the strain, $W(\mathbf{e})$, by $\mathbf{T}(\mathbf{e}) = (\mathbf{I} - 2\mathbf{e})\partial_{\mathbf{e}} W(\mathbf{e})$. Using (3.16), and (3.36) we get that

$$\mathbf{T}(\mathbf{e}) = \mu(\mathbf{I} - 2\mathbf{e})^{-1} - p\mathbf{I}, \tag{3.37}$$

where p is the Lagrange Multiplier enforcing incompressibility.

3.3.1 Semi-Inverse Approach

We will model the artery as a cylindrical tube with an inner radius r_i, and an outer radius r_o where points along the wall satisfy $r_i < r < r_o$. We will use a Semi-Inverse approach to find the components of the Cauchy stress tensor, $\mathbf{T}$, by assuming a general axisymmetric form for the displacement, $\tilde{\mathbf{u}}$, in the current configuration and then finding the stress by satisfying equilibrium and certain boundary conditions. In our case we use the standard axisymmetric form for displacement given by

$$\tilde{\mathbf{u}}((r, \theta, z)) = \eta(r)\mathbf{j}_1(\theta) + \lambda z \mathbf{j}_3, \tag{3.38}$$

Here, $\{\mathbf{j}_1(\theta), \mathbf{j}_2(\theta)\ , \mathbf{j}_3\}$ is the usual cylindrical basis with $\mathbf{j}_1(\theta) = \cos(\theta)\tilde{e}_1 + \sin(\theta)\tilde{e}_2$, $\mathbf{j}_2(\theta) = -\sin(\theta)\tilde{e}_1 + \cos(\theta)\tilde{e}_2$ and $\mathbf{j}_3 = \tilde{e}_3$ where $\{\tilde{e}_1, \tilde{e}_2, \tilde{e}_3\}$ is the standard basis in Cartesian coordinates.

Let $\mathbf{h} = \textbf{grad}\ \tilde{\mathbf{u}}$. Recall from (3.2) that $\mathbf{F} = (\mathbf{I} - \mathbf{h})^{-1}$. So that $\mathbf{B}^{-1} = \mathbf{F}^{-\mathrm{T}}\mathbf{F}^{-\mathbf{1}}$ implies that

$$\mathbf{B}^{-1} = (\mathbf{I} - \mathbf{h})^{\mathrm{T}}(\mathbf{I} - \mathbf{h}) = \mathbf{I} - (\mathbf{h}^{\mathrm{T}} + \mathbf{h}) + \mathbf{h}^{\mathrm{T}}\mathbf{h}. \tag{3.39}$$

With some minipulation we see that

$$\mathbf{I} - \mathbf{B}^{-1} = \mathbf{h}^{\mathrm{T}} + \mathbf{h} - \mathbf{h}^{\mathrm{T}}\mathbf{h}. \tag{3.40}$$

Therefore, (3.4) and (3.40) imply that

$$\mathbf{e} = \frac{1}{2}(\mathbf{h} + \mathbf{h}^{\mathrm{T}} - \mathbf{h}^{\mathrm{T}}\mathbf{h}). \tag{3.41}$$

The gradient, in cylindrical coordinates, of a vector valued function, $\mathbf{v} = \mathbf{v}_r\mathbf{j}_1(\theta) + \mathbf{v}_\theta\mathbf{j}_2(\theta) + \mathbf{v}_z\mathbf{j}_3$, is given by

$$\begin{aligned}\nabla_{r,\theta,z}\mathbf{v} = {} & \frac{\partial \mathbf{v}_r}{\partial r}\mathbf{j}_1(\theta)\otimes\mathbf{j}_1(\theta) + \frac{1}{r}(\frac{\partial \mathbf{v}_r}{\partial \theta} - \mathbf{v}_\theta)\mathbf{j}_1(\theta)\otimes\mathbf{j}_2(\theta) + \frac{\partial \mathbf{v}_r}{\partial z}\mathbf{j}_1(\theta)\otimes\mathbf{j}_3 \\ & + \frac{\partial \mathbf{v}_\theta}{\partial r}\mathbf{j}_2(\theta)\otimes\mathbf{j}_1(\theta) + \frac{1}{r}(\frac{\partial \mathbf{v}_\theta}{\partial \theta} + \mathbf{v}_r)\mathbf{j}_2(\theta)\otimes\mathbf{j}_2(\theta) + \frac{\partial \mathbf{v}_\theta}{\partial z}\mathbf{j}_2(\theta)\otimes\mathbf{j}_3 \\ & + \frac{\partial \mathbf{v}_z}{\partial r}\mathbf{j}_3\otimes\mathbf{j}_1(\theta) + \frac{1}{r}\frac{\partial \mathbf{v}_z}{\partial \theta}\mathbf{j}_3\otimes\mathbf{j}_2(\theta) + \frac{\partial \mathbf{v}_z}{\partial z}\mathbf{j}_3\otimes\mathbf{j}_3\end{aligned} \tag{3.42}$$

Applying (3.42), we have that $\mathbf{h}$ and $\mathbf{h}^{\mathrm{T}}$ are given respectively by

$$\begin{aligned}\mathbf{h} = {} & \eta'\mathbf{j}_1(\theta)\otimes\mathbf{j}_1(\theta) + \frac{\eta}{r}\mathbf{j}_2(\theta)\otimes\mathbf{j}_2(\theta) \\ & + \lambda\mathbf{j}_3\otimes\mathbf{j}_3\end{aligned} \tag{3.43}$$

and

$$\begin{aligned}\mathbf{h}^{\mathrm{T}} = {} & \eta'\mathbf{j}_1(\theta)\otimes\mathbf{j}_1(\theta) + \frac{\eta}{r}\mathbf{j}_2(\theta)\otimes\mathbf{j}_2(\theta) \\ & + \lambda\mathbf{j}_3\otimes\mathbf{j}_3.\end{aligned} \tag{3.44}$$

We also see that multiplying the two gives

$$\mathbf{h}^{\mathrm{T}}\mathbf{h} = \eta'^2\mathbf{j}_1(\theta)\otimes\mathbf{j}_1(\theta) + \frac{\eta^2}{r^2}\mathbf{j}_2(\theta)\otimes\mathbf{j}_2(\theta) \tag{3.45}$$

$$+ \lambda^2\mathbf{j}_3\otimes\mathbf{j}_3,$$

where $()' = \frac{\partial()}{\partial r}$. Substituting (3.43), (3.44) and (3.45) into (3.41), we have

$$2\mathbf{e} = (2\eta' - \eta'^2)\mathbf{j}_1(\theta)\otimes\mathbf{j}_1(\theta) \tag{3.46}$$

$$+ (\frac{2\eta}{r} - \frac{\eta^2}{r^2})\mathbf{j}_2(\theta)\otimes\mathbf{j}_2(\theta)$$

$$+ (2\lambda - \lambda^2)\mathbf{j}_3\otimes\mathbf{j}_3,$$

which implies that

$$(\mathbf{I} - 2\mathbf{e}) = (\eta' - 1)^2\mathbf{j}_1(\theta)\otimes\mathbf{j}_1(\theta) + (\frac{\eta}{r} - 1)^2\mathbf{j}_2(\theta)\otimes\mathbf{j}_2(\theta) \tag{3.47}$$

$$+ (\lambda - 1)^2\mathbf{j}_3\otimes\mathbf{j}_3,$$

or

$$(\mathbf{I} - 2\mathbf{e})^{-1} = \frac{1}{(\eta' - 1)^2}\mathbf{j}_1(\theta)\otimes\mathbf{j}_1(\theta) + \frac{1}{(\frac{\eta}{r} - 1)^2}\mathbf{j}_2(\theta)\otimes\mathbf{j}_2(\theta) \tag{3.48}$$

$$+ \frac{1}{(\lambda - 1)^2}\mathbf{j}_3\otimes\mathbf{j}_3.$$

Recall from (3.37) that the Cauchy stress tensor, with respect to the spatial strain tensor $\mathbf{e}$, is given as $\mathbf{T}(\mathbf{e}) = \mu(\mathbf{I} - 2\mathbf{e})^{-1} - p\mathbf{I}$. Therefore, (3.48) implies that the radial, circumferential and axial components of the Cauchy stress tensor are then given respectively by

the following equations:

$$\mathbf{T}_{rr}(r) = \mu(\eta' - 1)^{-2} - p(r), \tag{3.49}$$

$$\mathbf{T}_{\theta\theta}(r) = \mu(\frac{\eta}{r} - 1)^{-2} - p(r), \tag{3.50}$$

and

$$\mathbf{T}_{zz}(r) = \mu(\lambda - 1)^{-2} - p(r). \tag{3.51}$$

In section 3.2 we introduced a treatment of residual stress posed by Gorb and Walton that we modified to fit our model. Recall that in our formulation we can interchange $\mathbf{C}$ and $\mathbf{B}$. Therefore, we have that the stress-strain relation incorporating residual stress is given by

$$\hat{\mathbf{T}} = \mathbf{F_R}^{\mathrm{T}}(\mathbf{I} - 2\mathbf{e})\mathbf{F_R}\partial_{\mathbf{e}}W(\mathbf{e}). \tag{3.52}$$

Applying this notion of residual stress in the current configuration gives the radial, circumferential, and axial components, respectively, of the Cauchy stress tensor as:

$$\mathbf{T}_{rr}(r) = \mu(f_R)^2_{rr}(\eta' - 1)^{-2} - p(r), \tag{3.53}$$

$$\mathbf{T}_{\theta\theta}(r) = \mu(f_R)^2_{\theta\theta}(\frac{\eta}{r} - 1)^{-2} - p(r), \tag{3.54}$$

and

$$\mathbf{T}_{zz}(r) = \mu(f_R)^2_{zz}(\lambda - 1)^{-2} - p(r), \tag{3.55}$$

In (3.53), (3.54) and (3.55) $(f_R)_{rr}$, $(f_R)_{\theta\theta}$, and $(f_R)_{zz}$ are the radial, circumferential, and axial components of $\mathbf{F_R}$ respectively. As mentioned in section 3.2 we used a Fung split-ring paradigm for the deformation gradient $\mathbf{F_R}$ associated with a deformation from the cut-ring configuration to the intact unloaded residually stressed configuration. The form we take for $\mathbf{F_R}$ comes from Humphrey's book on cardiovascular solid mechanics [35]. In particular, consider a material point located at (R,Θ,Z), in the center region of a radially cut arterial segment, that gets mapped to (ρ,ϑ,ζ), in the center region of the intacted, unloaded and residually stressed configuration. The Cauchy stress tensor that arises from solving the boundary value problem with zero traction at the inner and outer boundaries is considered to be the residual stress distribution, and the gradient of the deformation that goes from the cut-ring configuration to the intact unloaded configuration is $\mathbf{F_R}$. In the book, the mapping used is given by

$$\rho = \rho(R), \quad \vartheta = \frac{\pi}{\Theta_o}\Theta, \quad \zeta = \Lambda Z \tag{3.56}$$

where Θ_o is the opening angle and Λ is the stretch ratio associated with residual stress. Note that $\Theta_o = \pi$ and $\Lambda = 1$ correspond to no residual stress. We use $\Theta_o = 100^\circ$ [34] and $\Lambda = 1.017695$ [35]. The components of $\mathbf{F_R}$ are then

$$\mathbf{F}_{\rho\rho} = \frac{\partial \rho}{\partial R}, \tag{3.57}$$

$$\mathbf{F}_{\vartheta\vartheta} = \frac{\rho\pi}{R\Theta_o} \tag{3.58}$$

and

$$\mathbf{F}_{\zeta\zeta} = \Lambda. \tag{3.59}$$

Incompressibility requires that $\det \mathbf{F_R} = 1$, so that

$$\frac{\partial \rho}{\partial R} = \frac{\Theta_o R}{\pi \Lambda \rho}, \tag{3.60}$$

which leads to

$$R = \left[R_o^2 - \frac{(\rho_o^2 - \rho^2)\pi\Lambda}{\Theta_o} \right]^{1/2}, \tag{3.61}$$

where R_o and rho_o are the outer radii for the cut-ring configuration and the intact unloaded configuration respectively. The components then become

$$\mathbf{F}_{\rho\rho} = \frac{\Theta_o R}{\pi \Lambda \rho}, \tag{3.62}$$

$$\mathbf{F}_{\vartheta\vartheta} = \frac{\rho\pi}{R\Theta_o} \tag{3.63}$$

and

$$\mathbf{F}_{\zeta\zeta} = \Lambda. \tag{3.64}$$

The point located at (ρ,ϑ,ζ) is then mapped to (r,θ,z), in the loaded current configuration. Pulling the components of $\mathbf{F_R}$ into the current loaded configuration, we have

$$(f_R)_{rr} = \frac{\Theta_o R(\rho(r))}{\pi \Lambda \rho(r)}, \tag{3.65}$$

$$(f_R)_{\theta\theta} = \frac{\rho(r)\pi}{R(\rho(r))\Theta_o} \tag{3.66}$$

and

$$(f_R)_{zz} = \Lambda, \tag{3.67}$$

where $\rho(r) = r - \eta(r)$.

Note that in (3.53), (3.54), and (3.55) we can solve for $p(r)$ using specified boundary conditions and satisfying the equations of motion, Div$\mathbf{T} = \mathbf{0}$, given in polar coordinates by

$$\frac{\partial \mathbf{T}_{rr}}{\partial r} + \frac{1}{r}\frac{\partial \mathbf{T}_{\theta r}}{\partial \theta} + \frac{\partial \mathbf{T}_{zr}}{\partial z} + \frac{\mathbf{T}_{rr} - \mathbf{T}_{\theta\theta}}{r} = 0 \tag{3.68}$$

$$\frac{\partial \mathbf{T}_{r\theta}}{\partial r} + \frac{1}{r}\frac{\partial \mathbf{T}_{\theta\theta}}{\partial \theta} + \frac{\partial \mathbf{T}_{z\theta}}{\partial z} + \frac{2\mathbf{T}_{r\theta}}{r} = 0 \tag{3.69}$$

$$\frac{\partial \mathbf{T}_{rz}}{\partial r} + \frac{1}{r}\frac{\partial \mathbf{T}_{\theta z}}{\partial \theta} + \frac{\partial \mathbf{T}_{zz}}{\partial z} + \frac{\mathbf{T}_{rz}}{r} = 0 \tag{3.70}$$

Note that, in this case, $\mathbf{T}$ is a diagonal matrix, and that $\mathbf{T}_{\theta\theta}$ and $\mathbf{T}_{zz}$ have no θ and z dependency respectively. Therefore, equations (3.69) and (3.70) are automatically satisfied and equation (3.68) becomes,

$$\frac{\partial \mathbf{T}_{rr}}{\partial r} + \frac{\mathbf{T}_{rr} - \mathbf{T}_{\theta\theta}}{r} = 0. \tag{3.71}$$

Manipulating (3.68) and then integrating from r_i to some point $r \in [r_i, r_o]$ together with the boundary boundary condition $\mathbf{T}_{rr}(r_i) = -P_i$ gives,

$$\mathbf{T}_{rr}(r) = \int_{r_i}^{r} \frac{\mathbf{T}_{\theta\theta} - \mathbf{T}_{rr}}{r} \partial r - P_i \tag{3.72}$$

Recall that equation (3.53) gives the form for $\mathbf{T}_{rr}(r)$ as $\mathbf{T}_{rr}(r) = \mu(f_R)_{rr}^2(\eta' - 1)^{-2} - p(r)$. Therefore, if we substitute that expression into (3.72) we will get the following

equation:

$$\int_{r_i}^{r} \frac{\mathbf{T}_{\theta\theta} - \mathbf{T}_{rr}}{r} \partial r - P_i = \mu (f_R)_{rr}^2 (\eta' - 1)^{-2} - p(r) \tag{3.73}$$

Solving for the Lagrange multiplier, $p(r)$, gives

$$p(r) = \mu (f_R)_{rr}^2 (\eta' - 1)^{-2} - \int_{r_i}^{r} \frac{\mathbf{T}_{\theta\theta} - \mathbf{T}_{rr}}{r} \partial r + P_i. \tag{3.74}$$

The only term still to solve for is the radial component of the displacement gradient, $\eta(r)$, which we will find using the incompressibility property of arteries.

Incompressibility means that volume is preserved. Mathematically, incompressibility requires that $\det (\mathbf{I} - 2\mathbf{e})^{-1} = 1$ as the determinent is a measure of volume change, and if the determinent is equal to one then there is no volume change. From (3.48) we have that

$$\det (\mathbf{I} - 2\mathbf{e})^{-1} = \frac{1}{(\eta' - 1)^2 (\frac{\eta}{r} - 1)^2 (\lambda - 1)^2}, \tag{3.75}$$

therefore, incompressibility implies that

$$\frac{1}{(\eta' - 1)^2 (\frac{\eta}{r} - 1)^2 (\lambda - 1)^2} = 1. \tag{3.76}$$

Letting $\tilde{\eta}(r) = \eta(r) - r$, then (3.76) becomes

$$\frac{1}{(\tilde{\eta}')^2 (\frac{\tilde{\eta}}{r})^2 (\lambda - 1)^2} = 1. \tag{3.77}$$

Manipulating (3.77) gives,

$$\frac{-r}{(\lambda - 1)} = (\tilde{\eta}\tilde{\eta}'). \tag{3.78}$$

Note that $-r$ can be rewritten as $-r = -(r^2/2)'$ and that $(\tilde{\eta}\tilde{\eta}')$ can be rewritten as $(\tilde{\eta}\tilde{\eta}') = (\tilde{\eta}^2/2)'$. Therefore, we can substitute those expressions into equation (3.78) and it follows

that we get the equation below:

$$\frac{-(\frac{r^2}{2})'}{(\lambda-1)} = \Big(\frac{\tilde{\eta}^2}{2}\Big)'. \tag{3.79}$$

Integrating this and taking square roots implies that

$$\tilde{\eta} = -\sqrt{\frac{c-r^2}{(\lambda-1)}}, \tag{3.80}$$

which from the definition of $\tilde{\eta}$, leads to

$$\eta(r) = r - \sqrt{\frac{c-r^2}{(\lambda-1)}}, \tag{3.81}$$

where c is an integration constant. If we assume no radial displacement on the outer wall, then we have $\eta(r_o) = 0$ which gives $c = r_0^2\lambda$. The displacement boundary condition that $\eta(r)$ is zero on the inner wall is not likely what would be observed physically. However, we use this assumption for illustrative purposes and it is not unreasonable. The final form of the radial displacement is then

$$\eta = r - \sqrt{\frac{r_o^2\lambda - r^2}{(\lambda-1)}}. \tag{3.82}$$

3.4 Using an Anisotropic Constitutive Relation

In this section we use an anisotropic constitutive form for the strain energy function W. In fact, we take the scalar function W in (3.28) to be the Helmholtz free energy function Ψ and use a constitutive relation posed by Holzapfel and Ogden [34]. Their relation assumes that the arterial wall is orthotropic with two fiber familes. We note that this form has been shown to be flawed if the properties of the fiber families differ [15]. However, for our case, the properties of the fibers do not differ. In their paper, they split Ψ additively into two parts consisting of an isotropic part and an anisotropic contribution. Therefore, they define

Ψ as

$$\Psi(\mathrm{I}_1, \mathrm{I}_4, \mathrm{I}_6) = \Psi_{iso}(\mathrm{I}_1) + \Psi_{aniso}(\mathrm{I}_4, \mathrm{I}_6), \tag{3.83}$$

where $\Psi_{iso}(\mathrm{I}_1)$ is the isotropic contribution to the energy and $\Psi_{aniso}(\mathrm{I}_4, \mathrm{I}_6)$ is the anisotropic contribution due to the collagen fibers. Also, I_1, I_4 and I_6 are material invariants given as

$$\mathrm{I}_1 = \mathrm{tr}\mathbf{C}; \quad \mathrm{I}_4 = \mathbf{C} \cdot \mathbf{A}_1; \quad \mathrm{I}_6 = \mathbf{C} \cdot \mathbf{A}_2 \tag{3.84}$$

where $\mathbf{A}_1 = \mathbf{a}_1 \otimes \mathbf{a}_1$ and $\mathbf{A}_2 = \mathbf{a}_2 \otimes \mathbf{a_2}$. Here we take $\mathbf{a}_1 = \mathbf{F_R}\bar{\mathbf{a}}_1$ and $\mathbf{a}_2 = \mathbf{F_R}\bar{\mathbf{a}}_2$. Here $\bar{\mathbf{a}}_1$, given by

$$\bar{\mathbf{a}}_1 = \begin{pmatrix} 0 \\ \cos\beta \\ \sin\beta \end{pmatrix} \tag{3.85}$$

and $\bar{\mathbf{a}}_2$, given by

$$\bar{\mathbf{a}}_2 = \begin{pmatrix} 0 \\ \cos\beta \\ -\sin\beta \end{pmatrix} \tag{3.86}$$

are the reference unit vectors in the fiber directions which correspond to what the authors call $\mathbf{a}_1$ and $\mathbf{a}_2$ respectively. In (3.85) and (3.86) β is the angle between the fibers which they take to be 29°.

Holzapfel and Ogden use a neo-hookean model for Ψ_{iso}

$$\Psi_{iso}(\mathrm{I}_1) = \frac{c}{2}(\mathrm{I}_1 - 3), \tag{3.87}$$

and a Fung exponential model for Ψ_{aniso}

$$\Psi_{aniso}(\mathrm{I}_4, \mathrm{I}_6) = \frac{k_1}{2k_2} \sum_{i=4,6} \{\mathbf{exp}[k_2(\mathrm{I_i} - 1)^2] - 1\} \tag{3.88}$$

Here $k_1 = 2.3632$kPa and $k_2 = 0.8393$. After transforming (3.87) and (3.88) into the current configuration we have

$$\Psi_{iso}(\mathbf{d}) = \frac{c}{2}(\mathrm{tr}(\mathbf{I} - 2\mathbf{d})^{-1} - 3) \tag{3.89}$$

and

$$\Psi_{aniso}(\mathbf{d}) = \frac{k_1}{2k_2} \sum_{i=1,2} \{\mathbf{exp}[k_2([(\mathbf{I} - 2\mathbf{d})^{-1}] \cdot \mathbf{A}_i - 1)^2] - 1\}. \tag{3.90}$$

We will find the gradients $\partial_{\mathbf{d}}\Psi_{iso}(\mathbf{d})$ and $\partial_{\mathbf{d}}\Psi_{aniso}(\mathbf{d})$ separately and then note that $\partial_{\mathbf{d}}\Psi(\mathbf{d}) = \partial_{\mathbf{d}}\Psi_{iso}(\mathbf{d}) + \partial_{\mathbf{d}}\Psi_{aniso}(\mathbf{d})$. To start, we consider $\partial_{\mathbf{d}}\Psi_{iso}(\mathbf{d})$. The gradient $\partial_{\mathbf{d}}\Psi_{iso}(\mathbf{d})$ is defined implicitly as the unique second order tensor satisfying,

$$\partial_{\mathbf{d}}\Psi_{iso}(\mathbf{d}) \cdot \mathbf{H} = \mathsf{D}_{\mathbf{d}}\Psi_{iso}(\mathbf{d})[\mathbf{H}], \quad \forall \mathbf{H} \in \mathfrak{T}^2 \tag{3.91}$$

Using (3.33) and (3.8),which define the derivatives for the trace of a second order tensor and the inverse of a second order tensor respectively, we have

$$\mathsf{D}_{\mathbf{d}}\Psi_{iso}(\mathbf{d})[\mathbf{H}] = \frac{c}{2}\text{tr}(-(\mathbf{I} - 2\mathbf{d})^{-1}(-2\mathbf{H})(\mathbf{I} - 2\mathbf{d})^{-1}). \tag{3.92}$$

Recalling that, for $\mathbf{A}$ and $\mathbf{B}$ in $\mathfrak{T}^2$, $\mathbf{A} \cdot \mathbf{B} = \text{tr}(\mathbf{A}^{\mathrm{T}}\mathbf{B})$ we see that,

$$\begin{aligned} \mathsf{D}_{\mathbf{d}}\Psi_{iso}(\mathbf{d})[\mathbf{H}] &= c(\mathbf{I} - 2\mathbf{d})^{-2} \cdot \mathbf{H} \\ &= \partial_{\mathbf{d}}\Psi_{iso}(\mathbf{d}) \cdot \mathbf{H} \end{aligned} \tag{3.93}$$

Therefore, we must have that,

$$\partial_{\mathbf{d}}\Psi_{iso}(\mathbf{d}) = c(\mathbf{I} - 2\mathbf{d})^{-2} \tag{3.94}$$

We will now find $\partial_{\mathbf{d}}\Psi_{aniso}(\mathbf{d})$. Rewriting (3.90) gives,

$$\Psi_{aniso}(\mathbf{d}) = \frac{k_1}{2k_2} \sum_{i=1,2} \{\mathbf{exp}[k_2(\text{tr}[(\mathbf{I} - 2\mathbf{d})^{-1}\mathbf{A}_i] - 1)^2] - 1\}. \tag{3.95}$$

Then using (3.33) and (3.8) again we have that,

$$\begin{aligned}\mathsf{D}_{\mathbf{d}}\Psi_{aniso}(\mathbf{d})[\mathbf{H}] = \frac{k_1}{2k_2}\sum_{i=1,2}\{2k_2(\text{tr}[(\mathbf{I}-2\mathbf{d})^{-1}\mathbf{A}_i]-1) \\ \times \mathbf{exp}[k_2(\text{tr}[(\mathbf{I}-2\mathbf{d})^{-1}\mathbf{A}_i]-1)^2] \\ \times \text{tr}(-(\mathbf{I}-2\mathbf{d})^{-1}(-2\mathbf{H})(\mathbf{I}-2\mathbf{d})^{-1}\mathbf{A}_i)\}\end{aligned} \tag{3.96}$$

Simplifying (3.96) gives,

$$\begin{aligned}\mathsf{D}_{\mathbf{d}}\Psi_{aniso}(\mathbf{d})[\mathbf{H}] = \Big[2k_1\sum_{i=1,2}\{(\text{tr}[(\mathbf{I}-2\mathbf{d})^{-1}\mathbf{A}_i]-1) \\ \times \mathbf{exp}[k_2(\text{tr}[(\mathbf{I}-2\mathbf{d})^{-1}\mathbf{A}_i]-1)^2] \\ \times [(\mathbf{I}-2\mathbf{d})^{-1}\mathbf{A}_i(\mathbf{I}-2\mathbf{d})^{-1}]\}\Big]\cdot\mathbf{H} \\ = \partial_{\mathbf{d}}\Psi_{aniso}(\mathbf{d})\cdot\mathbf{H}\end{aligned} \tag{3.97}$$

It follows that,

$$\begin{aligned}\partial_{\mathbf{d}}\Psi_{aniso}(\mathbf{d}) = 2k_1\sum_{i=1,2}\{(\text{tr}[(\mathbf{I}-2\mathbf{d})^{-1}\mathbf{A}_i]-1) \\ \times \mathbf{exp}[k_2(\text{tr}[(\mathbf{I}-2\mathbf{d})^{-1}\mathbf{A}_i]-1)^2] \\ \times [(\mathbf{I}-2\mathbf{d})^{-1}\mathbf{A}_i(\mathbf{I}-2\mathbf{d})^{-1}]\}\end{aligned} \tag{3.98}$$

Note that $\mathbf{A}_i = \mathbf{F}^{-1}\tilde{\mathbf{A}}_i$ where $\tilde{\mathbf{A}}_i = \tilde{\mathbf{a}}_i \otimes \tilde{\mathbf{a}}_i$ and $\tilde{\mathbf{a}}_i$ are vectors in the current fiber directions. This means that the $\mathbf{A}_i$'s are tensors with a spatial description. Therefore, using equation (3.98) and recalling from equation (3.94) that $\partial_{\mathbf{d}}\Psi_{iso}(\mathbf{d}) = c(\mathbf{I}-2\mathbf{d})^{-2}$, it follows that

the partial derivative, $\partial_{\mathbf{d}}\Psi(\mathbf{d})$, is given by

$$\begin{aligned}\partial_{\mathbf{d}}\Psi(\mathbf{d}) &= c((\mathbf{I}-2\mathbf{d}))^{-2} \\ &+ \Big[2k_1 \sum_{i=1,2}\{(\text{tr}[(\mathbf{I}-2\mathbf{d})^{-1}\mathbf{F_R}\mathbf{A}_i{\mathbf{F_R}}^{\text{T}}]-1) \\ &\times \mathbf{exp}[k_2(\text{tr}[(\mathbf{I}-2\mathbf{d})^{-1}\mathbf{F_R}\mathbf{A}_i{\mathbf{F_R}}^{\text{T}}]-1)^2] \\ &\times [(\mathbf{I}-2\mathbf{d})^{-1}\mathbf{A}_i(\mathbf{I}-2\mathbf{d})^{-1}]\}\Big].\end{aligned} \tag{3.99}$$

With the inclusion of residual stress, which was discussed in the previous section, we obtain the fo;;owing form for the isotropic part of the Helmholtz free energy:

$$(\Psi_{iso})_N(\mathbf{F}_R^{\text{T}}\mathbf{d}\mathbf{F}_R) = \frac{c}{2}\text{tr}[\mathbf{F}_R^{\text{T}}(\mathbf{I}-2\mathbf{d})^{-1}\mathbf{F}_R] \tag{3.100}$$

Recall that $\mathbf{F}_R$ is the gradient of the deformation that takes points from the cut-ring configuration to the intact residually stressed intermediate configuration, and whose radial, circumferential, and axial components are given respectively in (3.65), (3.66) and (3.67). Using similar calculations as above and noting that $\mathbf{F}_R$ is constant with respect to $\mathbf{d}$, we see that the partial derivative is given by

$$\partial_{\mathbf{d}}(\Psi_{iso})_N(\mathbf{F}_R^{\text{T}}\mathbf{d}\mathbf{F}_R) = c(\mathbf{I}-2\mathbf{d})^{-1}\mathbf{F}_R\mathbf{F}_R^{\text{T}}(\mathbf{I}-2\mathbf{d})^{-1} \tag{3.101}$$

Also, for the anisotropic part of the strain energy we have,

$$(\Psi_{aniso})_N(\mathbf{F}_R^{\text{T}}\mathbf{d}\mathbf{F}_R) = \frac{k_1}{2k_2}\sum_{i=1,2}\{\mathbf{exp}[k_2(\text{tr}[{\mathbf{F_R}}^{\text{T}}(\mathbf{I}-2\mathbf{d})^{-1}\mathbf{F_R}\mathbf{A}_i]-1)^2]-1\}. \tag{3.102}$$

Again, using similar calculations as above and noting that the tensor $\mathbf{F}_R$ is constant with respect to $\mathbf{d}$, we see that the partial derivative of the anisotropic part of the strain energy is

given by

$$\partial_{\mathbf{d}}(\Psi_{aniso})_N(\mathbf{F}_R^{\mathrm{T}}\mathbf{d}\mathbf{F}_R) = 2k_1 \sum_{i=1,2}\{(\mathrm{tr}[\mathbf{F_R}^{\mathrm{T}}(\mathbf{I}-2\mathbf{d})^{-1}\mathbf{F_R}\mathbf{A}_i]-1) \tag{3.103}$$

$$\times \mathbf{exp}[k_2(\mathrm{tr}[\mathbf{F_R}^{\mathrm{T}}(\mathbf{I}-2\mathbf{d})^{-1}\mathbf{F_R}\mathbf{A}_i]-1)^2]$$

$$\times [(\mathbf{I}-2\mathbf{d})^{-1}\mathbf{F_R}\mathbf{A}_i\mathbf{F_R}^{\mathrm{T}}(\mathbf{I}-2\mathbf{d})^{-1}]\}$$

The Cauchy stress tensor $\mathbf{T}$ becomes

$$\mathbf{T}(\mathbf{d}) = (\mathbf{I}-\mathbf{grad}\ \tilde{\mathbf{u}})^{\mathrm{T}}\partial_{\mathbf{d}}\big[\Psi_{iso}(\mathbf{F}_R^{\mathrm{T}}\mathbf{d}\mathbf{F}_R)+\Psi_{aniso}(\mathbf{F}_R^{\mathrm{T}}\mathbf{d}\mathbf{F}_R)\big](\mathbf{I}-\mathbf{grad}\ \tilde{\mathbf{u}}). \tag{3.104}$$

Substituting (3.101) and (3.103) into (3.104) gives,

$$\mathbf{T}(\mathbf{d}) = c(\mathbf{I}-\mathbf{grad}\ \tilde{\mathbf{u}})^{\mathrm{T}}(\mathbf{I}-2\mathbf{d})^{-1}\mathbf{F}_R\mathbf{F}_R^{\mathrm{T}}(\mathbf{I}-2\mathbf{d})^{-1}(\mathbf{I}-\mathbf{grad}\ \tilde{\mathbf{u}}) \tag{3.105}$$

$$+ (\mathbf{I}-\mathbf{grad}\ \tilde{\mathbf{u}})^{\mathrm{T}}\Big[2k_1 \sum_{i=1,2}\{(\mathrm{tr}[(\mathbf{I}-2\mathbf{d})^{-1}\mathbf{F_R}\mathbf{A}_i\mathbf{F_R}^{\mathrm{T}}]-1)$$

$$\times \mathbf{exp}[k_2(\mathrm{tr}[(\mathbf{I}-2\mathbf{d})^{-1}\mathbf{F_R}\mathbf{A}_i\mathbf{F_R}^{\mathrm{T}}]-1)^2]$$

$$\times [(\mathbf{I}-2\mathbf{d})^{-1}\mathbf{F_R}\mathbf{A}_i\mathbf{F_R}^{\mathrm{T}}(\mathbf{I}-2\mathbf{d})^{-1}]\}\Big](\mathbf{I}-\mathbf{grad}\ \tilde{\mathbf{u}}) - p\mathbf{I}.$$

Again, p is the Lagrange Multiplier enforcing incompressibility. We note here that the isotropic contribution to the Cauchy stress tensor $\mathbf{T}(\mathbf{d})$ is the same as in the isotropic constitutive relation case. This is because, as previously mentioed, with the assumptions we have made all matrices are diagonal so $\mathbf{d}$ and $\mathbf{e}$ have the same form.

3.4.1 Semi-Inverse Approach

Our formulations and assumptions are similar in this section as in 3.3.1. In particular we still model the artery as a cylindrical tube with an inner radius r_i, and an outer radius r_o where points along the wall satisfy $r_i < r < r_o$. We assume the same general axisymmetric form for the displacement, $\tilde{\mathbf{u}}$, given in (3.38), and then find the Cauchy stress by satisfying equilibrium and certain boundary conditions.

Recall that $\mathbf{h} = \mathbf{grad}\ \tilde{\mathbf{u}}$, and, from (3.2), that $\mathbf{F} = (\mathbf{I} - \mathbf{h})^{-1}$. So that $\mathbf{C}^{-1} = \mathbf{F}^{-\mathbf{1}}\mathbf{F}^{-\mathrm{T}}$ implies that

$$\begin{aligned} \mathbf{C}^{-1} &= (\mathbf{I} - \mathbf{h})(\mathbf{I} - \mathbf{h})^{\mathrm{T}} \\ &= \mathbf{I} - (\mathbf{h} + \mathbf{h}^{\mathrm{T}}) + \mathbf{h}\mathbf{h}^{\mathrm{T}}. \end{aligned} \tag{3.106}$$

With some minipulation we see that

$$\mathbf{I} - \mathbf{C}^{-1} = \mathbf{h} + \mathbf{h}^{\mathrm{T}} - \mathbf{h}\mathbf{h}^{\mathrm{T}}. \tag{3.107}$$

Therefore, (3.3) and (3.107) imply that

$$\mathbf{d} = \frac{1}{2}(\mathbf{h} + \mathbf{h}^{\mathrm{T}} - \mathbf{h}\mathbf{h}^{\mathrm{T}}), \tag{3.108}$$

where

$$\begin{aligned} \mathbf{h} = \mathbf{h}^{\mathrm{T}} &= \eta' \mathbf{j}_1(\theta) \otimes \mathbf{j}_1(\theta) + \frac{\eta}{r}\mathbf{j}_2(\theta) \otimes \mathbf{j}_2(\theta) \\ &+ \lambda \mathbf{j}_3 \otimes \mathbf{j}_3, \end{aligned} \tag{3.109}$$

Again, $\mathbf{h}$ is the same as in (3.43) as we are using the same form for the displacement. The

stress, $\mathbf{T}$, from (3.105) can be rewritten as

$$\begin{aligned}\mathbf{T}(\mathbf{d}) &= c(\mathbf{I}-\mathbf{h})^{\mathrm{T}}(\mathbf{I}-2\mathbf{d})^{-1}\mathbf{F}_R\mathbf{F}_R^{\mathrm{T}}(\mathbf{I}-2\mathbf{d})^{-1}(\mathbf{I}-\mathbf{h}) \\ &+ (\mathbf{I}-\mathbf{h})^{\mathrm{T}}\Big[2k_1\sum_{i=1,2}\{(\mathrm{tr}[(\mathbf{I}-2\mathbf{d})^{-1}\mathbf{F_R}\mathbf{A}_i\mathbf{F_R}^{\mathrm{T}}]-1) \\ &\times \mathbf{exp}[k_2(\mathrm{tr}[(\mathbf{I}-2\mathbf{d})^{-1}\mathbf{F_R}\mathbf{A}_i\mathbf{F_R}^{\mathrm{T}}]-1)^2] \\ &\times [(\mathbf{I}-2\mathbf{d})^{-1}\mathbf{F_R}\mathbf{A}_i\mathbf{F_R}^{\mathrm{T}}(\mathbf{I}-2\mathbf{d})^{-1}]\}\Big](\mathbf{I}-\mathbf{h}) - p\mathbf{I}.\end{aligned} \tag{3.110}$$

Noting that $\mathrm{tr}[(\mathbf{I}-2\mathbf{d})^{-1}\mathbf{F_R}\mathbf{A}_1\mathbf{F_R}^{\mathrm{T}}] = \mathrm{tr}[(\mathbf{I}-2\mathbf{d})^{-1}\mathbf{F_R}\mathbf{A}_2\mathbf{F_R}^{\mathrm{T}}]$, we can rewrite (3.110) as

$$\begin{aligned}\mathbf{T}(\mathbf{d}) &= (\mathbf{I}-\mathbf{h})^{\mathrm{T}}(\mathbf{I}-2\mathbf{d})^{-1}\mathbf{F}_R\Big[c\mathbf{I} \\ &+ 2k_1(\mathrm{tr}[(\mathbf{I}-2\mathbf{d})^{-1}\mathbf{F_R}\mathbf{A}_1\mathbf{F_R}^{\mathrm{T}}]-1) \\ &\times \mathbf{exp}[k_2(\mathrm{tr}[(\mathbf{I}-2\mathbf{d})^{-1}\mathbf{F_R}\mathbf{A}_1\mathbf{F_R}^{\mathrm{T}}]-1)^2] \\ &\times \big(\mathbf{A}_1+\mathbf{A}_2\big)\Big]\mathbf{F_R}^{\mathrm{T}}(\mathbf{I}-2\mathbf{d})^{-1}](\mathbf{I}-\mathbf{h}) - p\mathbf{I}.\end{aligned} \tag{3.111}$$

Also, from (3.108) and (3.109) we have that

$$\begin{aligned}(\mathbf{I}-2\mathbf{d})^{-1} &= (\eta'-1)^{-2}\mathbf{j}_1(\theta)\otimes\mathbf{j}_1(\theta) + (\frac{\eta}{r}-1)^{-2}\mathbf{j}_2(\theta)\otimes\mathbf{j}_2(\theta) \\ &+ (\lambda-1)^{-2}\mathbf{j}_3\otimes\mathbf{j}_3\end{aligned} \tag{3.112}$$

and

$$(\mathbf{I}-\mathbf{h}) = (\eta'-1)\mathbf{j}_1(\theta)\otimes\mathbf{j}_1(\theta) + (\frac{\eta}{r}-1)\mathbf{j}_2(\theta)\otimes\mathbf{j}_2(\theta) + (\lambda-1)\mathbf{j}_3\otimes\mathbf{j}_3. \tag{3.113}$$

Therefore, the radial, circumferential and axial components of stress take the forms:

$$\begin{aligned}\mathbf{T}_{rr}(r) = (f_R)^2_{rr}(\eta' - 1)^{-2}\Big[c \\ &+ 2k_1(\text{tr}[(\mathbf{I} - 2\mathbf{d})^{-1}\mathbf{F_R}\mathbf{A}_1{\mathbf{F_R}}^{\text{T}}] - 1) \\ &\times \mathbf{exp}[k_2(\text{tr}[(\mathbf{I} - 2\mathbf{d})^{-1}\mathbf{F_R}\mathbf{A}_1{\mathbf{F_R}}^{\text{T}}] - 1)^2] \\ &\times \big(\mathbf{A}_1(1,1) + \mathbf{A}_2(1,1)\big)\Big] - p(r)\end{aligned} \tag{3.114}$$

$$\begin{aligned}\mathbf{T}_{\theta\theta}(r) = (f_R)^2_{\theta\theta}(\frac{\eta}{r} - 1)^{-2}\Big[c \\ &+ 2k_1(\text{tr}[(\mathbf{I} - 2\mathbf{d})^{-1}\mathbf{F_R}\mathbf{A}_1{\mathbf{F_R}}^{\text{T}}] - 1) \\ &\times \mathbf{exp}[k_2(\text{tr}[(\mathbf{I} - 2\mathbf{d})^{-1}\mathbf{F_R}\mathbf{A}_1{\mathbf{F_R}}^{\text{T}}] - 1)^2] \\ &\times \big(\mathbf{A}_1(2,2) + \mathbf{A}_2(2,2)\big)\Big] - p(r)\end{aligned} \tag{3.115}$$

$$\begin{aligned}\mathbf{T}_{zz}(r) = (f_R)^2_{zz}(\lambda - 1)^{-2}\Big[c \\ &+ 2k_1(\text{tr}[(\mathbf{I} - 2\mathbf{d})^{-1}\mathbf{F_R}\mathbf{A}_1{\mathbf{F_R}}^{\text{T}}] - 1) \\ &\times \mathbf{exp}[k_2(\text{tr}[(\mathbf{I} - 2\mathbf{d})^{-1}\mathbf{F_R}\mathbf{A}_1{\mathbf{F_R}}^{\text{T}}] - 1)^2] \\ &\times \big(\mathbf{A}_1(3,3) + \mathbf{A}_2(3,3)\big)\Big] - p(r)\end{aligned} \tag{3.116}$$

As we did in section 3.3.1, we can solve for the lagrange multiplier, $p(r)$, by using specified boundary conditions and satisfying equilibrium. Recall that, in the absence of body forces, the equilibrium equations are given by $\text{Div}\mathbf{T} = \mathbf{0}$. As we saw before, this vector equation has three components, only one of which is not automatically satisfied.

Recall that the surviving equation can be written in polar coordinates as

$$\frac{\partial \mathbf{T}_{rr}}{\partial r} + \frac{1}{r}\frac{\partial \mathbf{T}_{\theta r}}{\partial \theta} + \frac{\partial \mathbf{T}_{zr}}{\partial z} + \frac{\mathbf{T}_{rr} - \mathbf{T}_{\theta\theta}}{r} = 0 \tag{3.117}$$

Again, this equation can be reduced to just

$$\frac{\partial \mathbf{T}_{rr}}{\partial r} + \frac{\mathbf{T}_{rr} - \mathbf{T}_{\theta\theta}}{r} = 0. \tag{3.118}$$

Manipulating (3.118) and then integrating from r_i to some point $r \in [r_i, r_o]$ together with the boundary condition $\mathbf{T}_{rr}(r_i) = -P_i$ gives,

$$\mathbf{T}_{rr}(r) = \int_{r_i}^{r} \frac{\mathbf{T}_{\theta\theta} - \mathbf{T}_{rr}}{r} \partial r - P_i. \tag{3.119}$$

Substituting (3.114) into (3.119) gives,

$$\begin{aligned} \int_{r_i}^{r} \frac{\mathbf{T}_{\theta\theta} - \mathbf{T}_{rr}}{r} \partial r - P_i = (f_R)_{rr}^2 (\eta' - 1)^{-2} \Big[c \\ + 2k_1 (\mathrm{tr}[(\mathbf{I} - 2\mathbf{d})^{-1} \mathbf{F_R} \mathbf{A}_1 \mathbf{F_R}^{\mathrm{T}}] - 1) \\ \times exp[k_2 (\mathrm{tr}[(\mathbf{I} - 2\mathbf{d})^{-1} \mathbf{F_R} \mathbf{A}_1 \mathbf{F_R}^{\mathrm{T}}] - 1)^2] \\ \times \big(\mathbf{A}_1(1,1) + \mathbf{A}_2(1,1) \big) \Big] - p(r). \end{aligned} \tag{3.120}$$

Solving for the Lagrange multiplier, $p(r)$, gives

$$\begin{aligned} p(r) = (f_R)_{rr}^2 (\eta' - 1)^{-2} \Big[c + 2k_1 (\mathrm{tr}[(\mathbf{I} - 2\mathbf{d})^{-1} \mathbf{F_R} \mathbf{A}_1 \mathbf{F_R}^{\mathrm{T}}] - 1) \\ \times exp[k_2 (\mathrm{tr}[(\mathbf{I} - 2\mathbf{d})^{-1} \mathbf{F_R} \mathbf{A}_1 \mathbf{F_R}^{\mathrm{T}}] - 1)^2] \\ \times \big(\mathbf{A}_1(1,1) + \mathbf{A}_2(1,1) \big) \Big] - \int_{r_i}^{r} \frac{\mathbf{T}_{\theta\theta} - \mathbf{T}_{rr}}{r} \partial r + P_i. \end{aligned} \tag{3.121}$$

Note that since we have assumed the same displacement as in section 3.3.1 that the radial component of the displacement $\eta(r)$ has already been determined. With a model for the arterial wall stress under pressure in both the isotropic and anisotropic cases, we will look at our model for how growth is affected by an increase in arterial pressure in the next chapter.

4. MODEL FOR GROWTH

4.1 Brief Overview of Previous Hypertension Growth Models

Recall that mechanobiology is the study of how mechanical stimulation evokes biological consequences. Also, by now we have established that arterial growth, specifically growth due to increased smooth muscle activity, is directly affected by mechanical changes. Whether one believes the mechanical influence is a change in the arterial wall stress, either shear or circumferential, or a change in strain, every arterial growth model should include a clear function for how growth, via an increase in mass, will be affected by some measure of either stress or strain. Furthermore, growth is a dynamic processes and the time scale is on the order of weeks to months as a result of the half-life of key wall constituents [55]. Therefore, any arterial growth model should also have a time-dependent growth law that defines the evolution of growth as a function of arterial stresses or strains. With these basic considerations in mind, we review a few models from the literature that model arterial growth due to an increase in arterial pressure, or hypertension.

There have been a number of papers addressing the issue of modeling arterial growth and adaptation [70, 58, 69, 20, 71, 29, 3, 1, 17, 38, 72, 16, 51, 60, 59, 67]. In particular, Taber and Eggers modeled growth due to hypertension using a growth law that depended linearly on the circumferential stress, however, they did not include any measure of mechanical homeostasis [70]. Where the popular idea of a homeostastic stress target is commonly considered the primary goal of growth and remodeling processes such as arterial growth. In contrast to this study, in a later work, Taber used a growth law that depended linearly on the the deviation of the circumferential component of wall stress from a constant homeostastic target [69]. Taber and Humphrey used a similarly model to describe general stress-mediated arterial growth [71]. Alford et at included the contractility of smooth

muscle cells to their stress-modulated model for growth due to sudden hypertension. They also modeled the artery as a mixture, using theories from Humphrey and Rajagopal's 2002 paper. Their growth law also included a perturbation of circumferential wall stress away from some constant homeostastic stress target [1]. All the models mentioned thus far in this section have used an extension of the volumetric growth theories of Rodriguez et al, with a consideration of growth and remodeling processes and, in most cases, mechanical homeostasis with the circumferential wall stress as the driving force for growth. In contrast to all of the aforementioned approaches, Saez et al used a purely volumetric concept of growth with a growth that was a constant growth criteria with no dependence on circumferential wall stress [67]. Aside from the fact that we do not use any form of volumetric growth, the way we model growth is different from this in that we have a growth law that is dependent on the circumferential wall stress and a notion of homeostasis, even for the bang-bang method where the the growth law is just a constant which is the maximum rate of growth. We also have a point-wise homeostastic stress distribution. Our growth model is discussed in detail below.

4.2 Current Growth Model

As previously mentioned, growth is assumed to occur in order to drive the arterial wall stress back to a normal "preferred" state. Thus we will model growth as a result of a perturbation of the circumferential wall stress away from some homeostatic stress measure. In particular, we take the preferred stress to be the circumferential stress distribution corresponding to a normal systolic blood pressure of 120 mm Hg. It is common in the hypertension induced growth modeling literature to assume that the homeostatic circumferential stress state is a constant, usually a through-the-wall average. In contrast, we take the homeostatic stress state to be that spatially inhomogeneous stress state corresponding to the normal systolic blood pressure of 120 mm Hg, thereby allowing for the

possibility that material gets added at different rates through the wall of the artery. Indeed, more growth occurs for radial positions closer to the inner wall. The function that dictates growth is defined as,

$$G(r) = \mathbf{Max}[0, \mathbf{T}^h(r) - (\mathbf{T}^p(r) + \epsilon)]. \tag{4.1}$$

In (4.1), $\mathbf{T}^h(r)$ is the circumferential wall stress distribution under hypertensive pressure and $\mathbf{T}^p(r)$ is the preferred circumferential wall stress distribution taken to be under normal pressure of 120 mmHg. We include the ϵ-band around the preferred stress distribution under the assumption that natural growth processes might not be able to return the stress distribution back to homeostasis but rather only to within an epsilon band of the desired state. Equation (4.1) implies that, at any point within the wall, if the hypertensive stress exceeds the ϵ-band around the preferred stress then growth occurs, otherwise there is no growth at that point. Therefore, $G(r)$ describes how much the current wall stress under hypertension differs from the homeostatic stress at each point through the thickness of the wall. Therefore, to return to homeostasis is to aim at driving $G(r)$ to zero for every point through the thickness of the wall. Moreover, since the most growth occurs at the inner wall, this will be accomplished when $G(r_i)$ is zero.

We consider the process of biological growth to be defined as the production of mass. Therefore we need to define how the change in stress will affect the mass production. We define the relative change in mass production over time as

$$\frac{\dot{m}(r,t)}{m(r,t_o)} = H(\mathbf{T}), \tag{4.2}$$

where

$$H(\mathbf{T}) = \frac{b_1 G(r)}{b_0 + G(r)}. \tag{4.3}$$

In equation (4.6), b_1 is based on the maximum mass production rate of smooth muscle cells during hypertension and changes depending on the initial stress at the onset of hypertension and on a specified value of b_0. For instance, we take the maximum relative rate of smooth muscle production to be $.84\%$/day at the unset of hypertension, and

$$b_1 = \frac{b_0}{G^{\mathbf{Max}}(r_i)} + 1, \tag{4.4}$$

where $G^{\mathbf{Max}}(r_i)$ is the maximum stress difference at the initial onset of hypertension. We chose $b_0 = 1000$ to control the rate at which material was being added in the continuous case. We solve (4.2) by using a forward difference method. Equation (4.6) infers that more mass is added in the initial stages followed by a gradual decrease. The model is one way to ensure that we do not have unbounded growth.

For the bang-bang case we use the same criteria for growth, however, the relative change of smooth muscle production is constant, in particular is $.0084$. We define the relative mass production as

$$\frac{\dot{m}(r,t)}{m(r,t_o)} = K(\mathbf{T}), \tag{4.5}$$

where

$$K(\mathbf{T}) = \begin{cases} 0 & G(r) = 0 \\ .0084 & G(r) \neq 0 \end{cases}. \tag{4.6}$$

We give a brief outline of our solution process in the next section.

4.3 Solution Process

We first note that for both the continuous and the bang-bang growth rates the solution process is similar, and therefore we will present an outline for the continuous case

only. Also, for illustrative purposes we will look only at the isotropic case, noting that the anisotropic case has a similar procedure. We consider time steps $[t_0, t_1, ..., t_{n-1}, t_n, ...]$ where t is measured in days and $\Delta t = 1$. We take $r_i(t_0)$, the initial inner radius at time t_0, to be 2.85mm [35]. Next, recall from section 3.3.1 that $\mathbf{T}_{\theta\theta}(r) = \mu(f_R)^2_{\theta\theta}(\frac{\eta}{r} - 1)^{-2} - p(r)$, where $p(r)$ was determined by satisfying equilibrium and the stress boundary condition $\mathbf{T}_{\theta\theta}(r_i(t_0)) = -P_i$. Therefore,

$$\begin{aligned}\mathbf{T}_{\theta\theta}(r;t_0) = \mu(f_R(r;t_0))^2_{\theta\theta}(\frac{\eta(r;t_0)}{r} - 1)^{-2} - \mu(f_R(r;t_0))^2_{rr}(\eta'(r;t_0) - 1)^{-2} \\ + \int_{r_i(t_0)}^{r} \frac{\mu(f_R(r;t_0))^2_{\theta\theta}(\frac{\eta(r;t_0)}{r} - 1)^{-2} - \mu(f_R(r;t_0))^2_{rr}(\eta'(r;t_0) - 1)^{-2}}{r}\partial r \\ - P_i.\end{aligned} \tag{4.7}$$

We then use 4.7 to determine $G(r;t_0)$ and in particular our initial maximum stress difference, $G(r_i(t_0);t_0)$. When r_i gets updated, we repeat this process. The general procedure for updating r_i is as follows: at each time step, we solve

$$\frac{\Delta m(r,t_n)}{m(r,t_o)} = \int_{r_i(t_{n-1})}^{r_o} \frac{\dot{m}(r,t_{n-1})}{m(r,t_o)}\Delta t_{n-1}\frac{r\partial r}{(r_o^2 - r_i^2(t_{n-1}))} \tag{4.8}$$

Then we have

$$r_i^2(t_{n-1}) - r_i^2(t_n) = \frac{\Delta m(r,t_n)}{m(r,t_o)}(r_o^2 - r_i^2(t_0)). \tag{4.9}$$

Finally, we have that

$$r_i(t_n) = \sqrt{r_i^2(t_{n-1}) - \frac{\Delta m(r,t_n)}{m(r,t_o)}(r_o^2 - r_i^2(t_0))}. \tag{4.10}$$

Note that density does not appear in (4.9) because we are assuming constant density, ρ_o. Also, because we keep the outer radius r_o fixed, the change in area is just $r_i^2(t_{n-1}) - r_i^2(t_n)$.

As mentioned above, once we have updated r_i we use it to update the circumferential component of the Cauchy stress and subsequently the maximum stress difference. Our results are presented in the following chapter.

5. RESULTS

5.1 Results for Isotropic Constitutive Relation

In this section we present results for the isotropic constitutive relational form for the strain energy function W. As mentioned in section 1.2, we will compare the results for a continuous growth model, where material is added in a continuous manner that varies with radial position through the arterial wall, and for a bang-bang growth model, where material is being added at a constant maximum rate. Recalling step five of Humphrey's five basic steps for constitutive formulations, we seek to test the predictive capability of our model, in particular, its ability to predict an increase in wall thickness during hypertension as a result of the perturbation of the circumferential component of wall stress from a preferred state of homeostasis. As noted in section 4.2, the most growth occurs at the inner wall, thus the stress will be farther away from homeostasis there and so $G(r_i)$ is the maximum of $G(r)$ at any given time. In order to gauge how well growth can return the circumferential hypertensive stress back to homeostasis, we track how long it takes growth to minimize the maximum stress difference, $G(r_i)$. We give results for the continuous and bang-bang cases below.

For the continuous case, Figure 5.1 shows how the maximum stress decreases as a function of time as a result of the thickening of the arterial wall. Over a long period of time, we can see that the value of $G(r_i)$ is approaching zero, which means that the stress returns to homeostasis asymptotically in time. Figure 5.2 shows by how much the wall of the artery is actually thickening as the stress is going down. The outer radius, r_o is fixed at 3.05mm and the inner radius, r_i, decreases from 2.85mm.

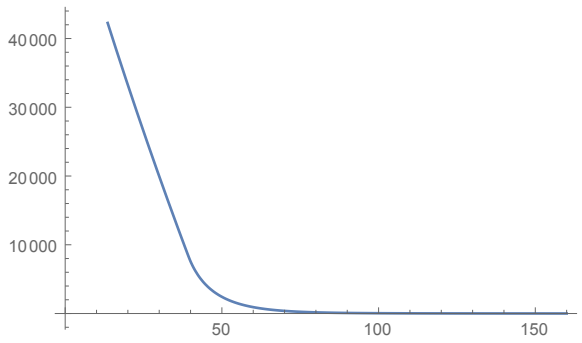

Figure 5.1: Max stress difference, $G(r_i)$, in Pa vs time in days for the continuous case using an isotropic model

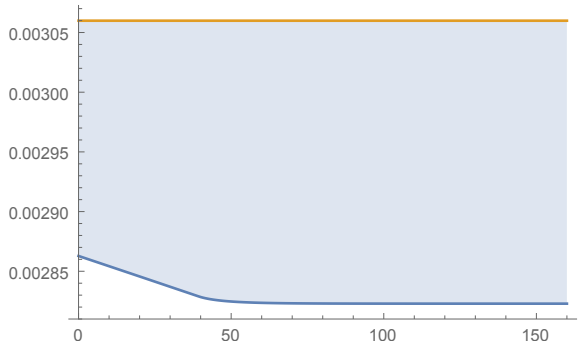

Figure 5.2: Artery thickness in meters vs time in days for the continuous case using an isotropic model

For the bang-bang case, Figures 5.3 and 5.4 show maximum stress, $G(r_i)$, decrease and wall thickening respectively. The results for the bang-bang are similar in that $G(r_i)$ still approaching zero as the stress returns to homeostasis; however, the bang-bang model takes less time to return to homeostasis. It is clear, and possibly expected, that the bang-bang method performs better as it is adding mass at a faster rate; however, it is interesting to note that between Figure 5.2 and Figure 5.4 there is little to no difference in the wall thickness. It appears that using the bang-bang method does not actually add more material but rather predicts the same amount of growth in a shorter period of time.

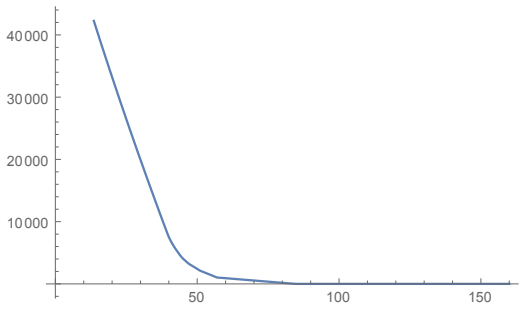

Figure 5.3: Max stress difference, $G(r_i)$, in Pa vs time in days for the bang-bang case using an isotropic model

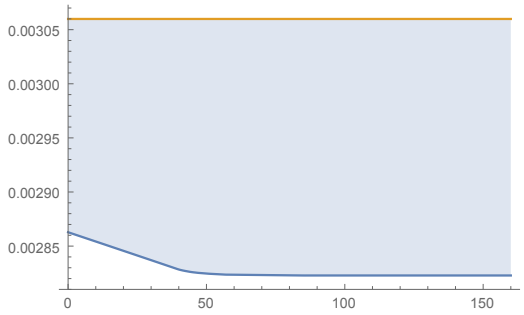

Figure 5.4: Artery thickness in meters vs time in days for the bang-bang case using an isotropic model

In the next section we present the results for the anisotropic case.

5.2 Results for Anisotropic Constitutive Relation

Here we provide results for the case when we assume an anisotropic modified Holzapfel-Ogden constitutive form for W. Figure 5.5 shows how the maximum stress, $G(r_i)$ decreases over time as a result of the wall of the artery thickening. We take the circumferential wall stress $\mathbf{T}^h(r)$ to be under a hypertensive systolic pressure of 140mmHg (≈ 19 kPa) and ϵ to be approximately 6 kPa, same as above.

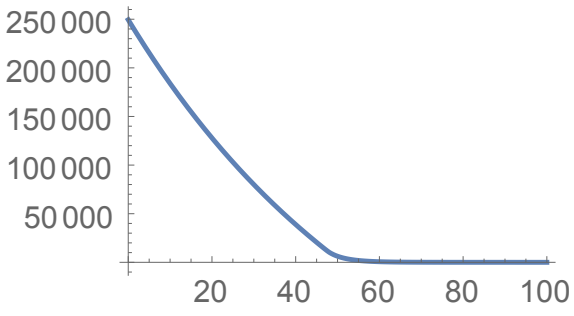

Figure 5.5: Max stress difference, $G(r_i)$, in Pa vs time in days for the continuous case using an anisotropic model

Again, as a function of time, t, we observe that $G(r_i) \to 0$ as $t \to \infty$ which means that the stress returns to homeostasis asymptotically in time. Figure 5.6 shows by how much the wall of the artery is actually thickening as the stress is going down. Again, we took the outer radius, r_o to be fixed at $3.05mm$ and the inner radius, r_i, to start at $2.85mm$.

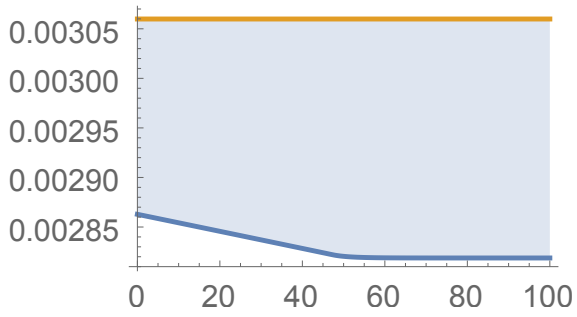

Figure 5.6: Artery thickness in meters vs time in days for the continuous case using an anisotropic model

We note that the isotropic contribution in the Holzapfel-Ogden constitutive relation is the same as in the purely isotropic case. Furthermore, the continuous method with the anisotropic contribution included performs better than that of the purely isotropic case, requiring less time to return to homeostasis. In particular, using the anisotropic model predicts a more efficient growth process. However, we observe that even when making comparisons between the isotropic and anisotropic cases, the wall thickness is approximately the same with either model.

Next we consider the results for the bang-bang method for controlling the rate at which material is added, which we recall assumes that whenever growth occurs material is added at a constant maximum rate. Figures 5.7 and 5.8 show $G(r_i)$ and wall thickness respectively over time using the bang-bang method. Again, we expect that because material is being added at a maximum rate we expect, and observe, that $G(r_i)$ will actually reach zero

and will do so in a relatively short amount of time as compared to the continuous case.

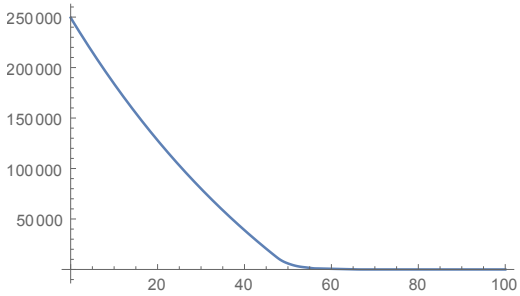

Figure 5.7: Max stress difference, $G(r_i)$, in Pa vs time in days for the bang-bang case using an anisotropic model

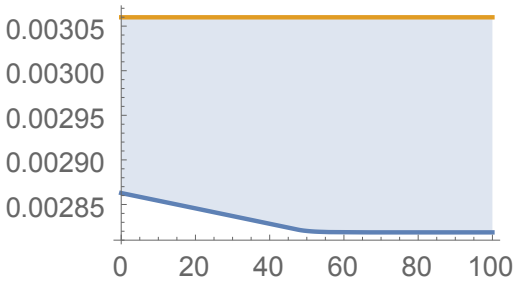

Figure 5.8: Artery thickness in meters vs time in days for the bang-bang case using an anisotropic model

As was the case with the isotropic constitutive relation, the artery has thickened by roughly the same amount with both the continuous and bang-bang growth rates.

The systolic blood pressure measure of 140mmHg is on the lower scale of hypertensive pressures, being closer to prehypertensive. We therefore wish to see how our model predicts the arterial wall response to severe high blood pressure. To that end, we increased the systolic blood pressure to 200mmHg and observed the results for both the continuous growth method and the bang-bang method. Figures 5.9 and 5.10 show the progression of $G(r_i)$ and wall thickness respectively.

From the graphs we can see that the time to return to homeostasis is much greater than with a hypertensive pressure of 140mmHg, in particular it takes more than twice the time to drive the maximum stress difference down with a pressure of 200mmHg. Figures 5.11 and 5.12 show $G(r_i)$ and thickness for the bang-bang method with an initial pressure of 200mmHg respectively.

The ϵ-band taken around the preferred stress $\mathbf{T}^p(r)$ was kept fixed in all of the previous cases. We took $\epsilon \approx 6$ kPa which corresponded to the difference between the average of

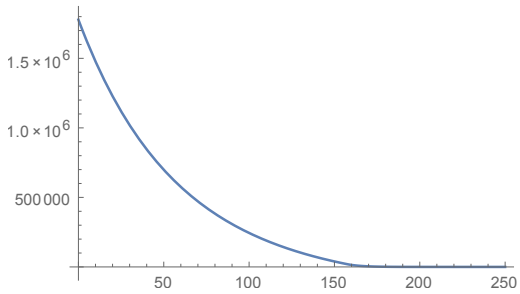

Figure 5.9: Max stress difference, $G(r_i)$, in Pa vs time in days for the continuous case with the pressure at 200mmHg

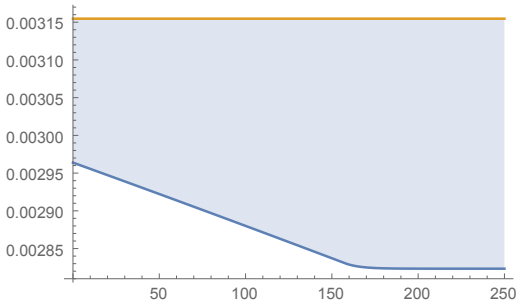

Figure 5.10: Artery thickness in meters vs time in days for the continuous case with the pressure at 200mmHg

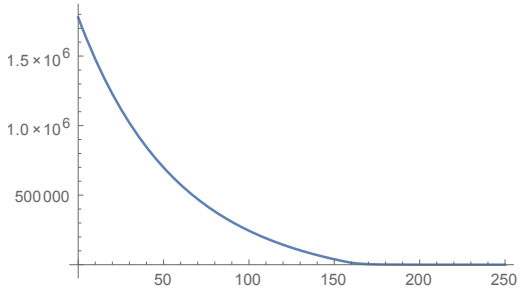

Figure 5.11: Max stress difference, $G(r_i)$, in Pa vs time in days for the bang-bang case with the pressure at 200mmHg

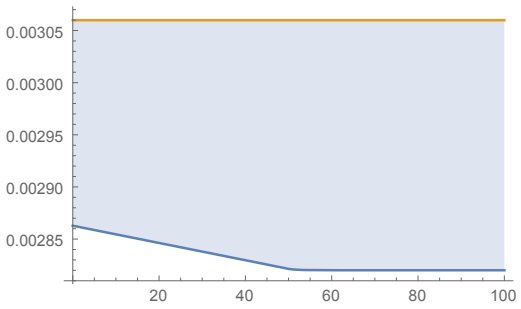

Figure 5.12: Artery thickness in meters vs time in days for the continuous case with the pressure at 200mmHg

the preferred wall stress at 120mmHg and the average of the wall stress at 125mmHg. Our next calculations focused on what would happen if we changed the ϵ-band size that we took around $\mathbf{T}^p(r)$. We increased the pressure of $\mathbf{T}^h(r)$ to 200mmHg and varied ϵ from 0kPa to about 23kPa which correspond to doing the process discussed above for pressures of 120mmHg to 140mmHg respectively. We plotted the final thickness of the wall when the stress returned back to homeostasis to within the given ϵ-band as a function of the size of the ϵ-band. We also plotted the time it took to complete this process as a function of the size of the ϵ-band. The results using both the continuous growth rate and

the bang-bang method are shown in the following figures. Figures 5.13 and 5.14 show results for the final thickness as a function of ϵ and for the final time as a function of ϵ for the continuous growth rate case respectively. Also, Figures 5.15 and 5.16 show results for the final thickness as a function of ϵ and for the final time as a function of ϵ for the bang-bang method respectively.

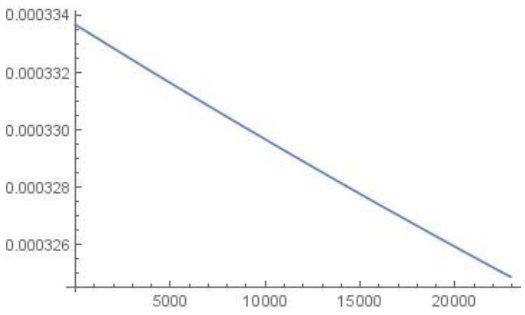

Figure 5.13: Final-thickness in $meters$ vs ϵ in *Pa* using a continuous growth rate

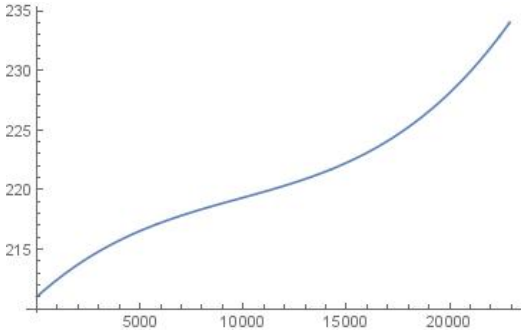

Figure 5.14: Final-time in *days* vs ϵ *Pa* using a continuous growth rate

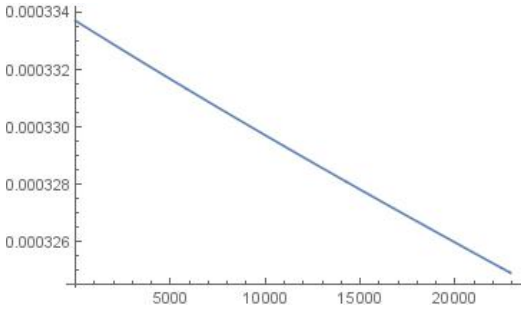

Figure 5.15: Final-thickness in $meters$ vs ϵ in *Pa* using the bang-bang method

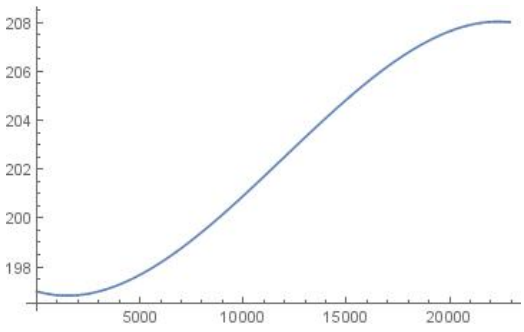

Figure 5.16: Final-time in *days* vs ϵ *Pa* using the bang-bang method.

In both the continuous and bang-bang cases the thickness is decreasing and the time is

increasing but as usual the bang-bang method does a better job, taking less time to return to homeostasis. It seems counter intuitive that the time would be increasing as the ϵ-band size gets bigger. Figures 5.17 and 5.18 show $G(r_i)$ for the four different ϵ-band sizes for the continuous case and the bang-bang method respectively.

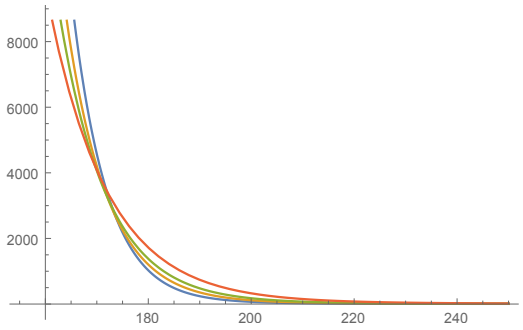

Figure 5.17: Max stress differences, $G(r_i)$, in Pa vs time in days for the continuous case for different ϵ-band sizes: the blue line is $G(r_i)$ with $\epsilon = 0$kPa; the orange line is $G(r_i)$ with $\epsilon = 6$kPa; the green line is $G(r_i)$ with $\epsilon = 11$kPa and the red line is $G(r_i)$ with $\epsilon = 23$kPa

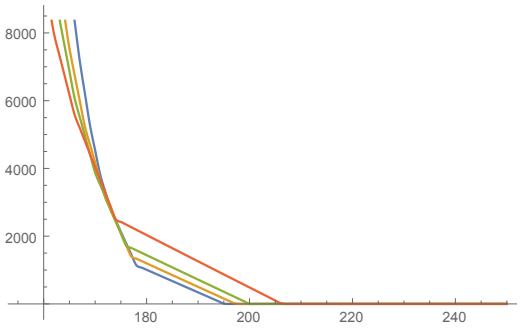

Figure 5.18: Max stress differences, $G(r_i)$, in Pa vs time in days for the bang-bang case for different ϵ-band sizes: the blue line is $G(r_i)$ with $\epsilon = 0$kPa; the orange line is $G(r_i)$ with $\epsilon = 6$kPa; the green line is $G(r_i)$ with $\epsilon = 11$kPa and the red line is $G(r_i)$ with $\epsilon = 23$kPa.

In both graphs, the blue lines represent $G(r_i)$ with $\epsilon = 0$kPa, the orange lines represent $G(r_i)$ with $\epsilon = 6$kPa, the green lines represent $G(r_i)$ with $\epsilon = 11$kPa and the red lines represent $G(r_i)$ with $\epsilon = 23$kPa. As the graphs indicate, the larger band size initially drives down the value of $G(r_i)$ faster than the smaller band size; however, after some time, smaller band size starts having lower values for $G(r_i)$. This appears to result in it taking longer to return to homeostasis with bigger band sizes. We conclude with some discussion in the following chapter.

6. DISCUSSION

We have discussed a way to formulate elasticity for both an isotropic and an anisotropic incompressible residually stressed material body in the current configuration. We used the formulations to determine stress-strain relations for both an isotropic and an anisotropic constitutive form for the strain energy W. We then calculated stresses using a semi-inverse approach that assumed axisymmetric deformation. We defined the evolution of growth to be a proportional function of the deviation of circumferential wall stress away from homeostasis, as well as a bang-bang method whose activation was dependent on whether or not the circumferential wall stress exceeded homeostatic levels. We then tested the predictive capability of our model to capture certain salient aspects of the arterial wall response to hypertension, namely the thickening of the arterial wall. Our model did suggest that arterial growth occurs to drive the circumferential wall stress back to homeostasis.

We started with a pre-hypertensive arterial pressure of 140mmHg and observed that the circumferential wall stress returned back to homeostasis to within ϵ, where $\epsilon \approx 6$kPa, asymptotically in time using both the continuous and the bang-bang growth rates as well as the isotropic and anisotropic models. When we used a bang-bang controller for the growth rate, in both the isotropic and anisotropic cases, the circumferential wall stress got within ϵ of the preferred stress in less time than the continuous case, with the lowest time being just under 60 days for the anisotropic case with a pre-hypertensive pressure of 140mmHg. However, in all cases, the amount of growth or final thickness of the arterial wall was the same.

We then increased the pressure to 200mmHg and varied the size of the ϵ-band we took around the preferred stress distribution $\mathbf{T}^p(r)$. The results showed that the larger the band size the longer it took for growth to drive down the maximum stress difference

$G(r_i)$. We also observed that when we increased the pressure to 200mmHg that it took more than twice as long to return to within ϵ of the homeostatic stress, even in the case of the bang-bang growth rate. Furthermore, the efficiency of the bang-bang method over the continuous case was also diminished with an increase in the hypertensive pressure from 140mmHg to 200mmHg. For instance, for a starting pressure of 140mmHg, the bang-bang method was 35% faster than the continuous growth rate, and only 20% faster than the continuous growth rate when we take a hypertensive pressure of 200mmHg. This observation suggests that, in the case of more severely high hypertensive pressures that growth alone may not be enough to return the stress to homeostasis. Indeed, we did exclude the effects of any remodeling processes present during hypertension. Humphrey and Rajagopal mentioned that growth and remodeling are often coupled processes, and at times it takes both types of responses to achieve mechanical homeostasis [40]. For example, the wall not only becomes thicker but also can become stiffer due mainly to the reorientation of structurally significant constituents in the arterial wall. In addition to remodeling effects, we also did not include many other biological complexities such as the multilayer structure of the arterial wall and any role elastin or collagen might play in the growth process (mass addition) during hypertension. While it would be relatively straightforward to incorporate such effects via mixture theory formulated in the current configuration, the biological issues surrounding understanding to what extent each of these biological processes contribute to adaptations leading to a return to homeostatic stresses and strains are quite complex and are far from being definitively agreed upon. We also assumed zero displacement on the outer wall of the artery when that is likely not the case. Although, in some respect, the bang-bang method is clearly optimal, it is important to note that we are not claiming that a bang-bang controller is the best way to model growth rate. In fact, we are simply considering two commonly used methods and see which one produces better results as far as which method is more time efficient, with the assumption that natural processes often will

favor a minimal method.

There is a need to continue developing continuum mechanics models, like this one, to study the mechanobiology of arterial diseases not only to aid in clinical treatment but also in surgical interventions [37]. For instance, the area of tissue engineering relies heavily on a working knowledge of growth and remodeling processes that can occur due to the introduction of a foreign object into the body [32]. A stent, for instance, is a medical instrument that is inserted into the lumenal area of an occluded artery to allow for proper blood flow to the rest of the body. It is important, therefore, to know what effect constant distention will have on the strength of the arterial wall. Such mechanobiological influences on the advancement of medical procedure and treatment can only exist with more collaboration between clinicians, mathematicians and biologists.

REFERENCES

[1] P. W. Alford, J. D. Humphrey, and Larry A. Taber. Growth and remodeling in a thick-walled artery model: effects of spatial variations in wall constituents. *Biomech Model Mechanobiol*, 7:245–262, 2008.

[2] D. Ambrosi, G. A. Ateshian, E. M. Arruda, S. C. Cowin, J. Dumais, A. Goriely, G. A. Holzapfel, J. D. Humphrey, R. Kemkemer, E. Kuhl, J. E. Olberding, L. A. Taber, and K. Garikipati. Perspectives on biological growth and remodeling. *J Mech Phys Solids*, 59:863–883, 2011.

[3] D. Ambrosi, A. Guillou, and E. S. DiMartino. Stress-modulated remodeling of a non-homogeneous body. *Biomech Model Mechanobiol*, 7:63–76, 2008.

[4] G. A. Ateshian. On the theory of reactive mixtures for modeling biological growth. *Biomech Model Mechanobiol*, 6:423–445, 2007.

[5] G. A. Ateshian and J. D. Humphrey. Continuum mixture models of biological growth and remodeling: past successes and future opportunities. *Annu Rev Biomed Eng*, 14:97–111, 2012.

[6] S. Baek and J. D. Humphrey. Computational modeling of growth and remodeling in biological soft tissues: application to arterial mechanics. In S. De et al, editor, *Computational Modeling in Biomechanics*. Springer Science+Business Media B.V., 2010.

[7] L. Cardamone, A. Valentin, J. F. Eberth, and J. D. Humphrey. Origin of axial pre-stress and residual stress in arteries. *Biomech Model Mechanobiol*, 2009.

[8] T. E. Carew, R. N. Vaishnav, and D. J. Patel. Compressibility of the arterial wall. *Circ Res*, 23:61–68, 1968.

[9] S. Chien, S. Li, and J. Y. L. Shyy. Effects of mechanical forces on signal transduction and gene expression in endothelial cells. *J Hypertension*, 31:62–69, 1998.

[10] C. J. Chuong and Y. C. Fung. Three-dimensional stress distribution in arteries. *J Biomech*, 105:268–274, 1983.

[11] C. J. Chuong and Y. C. Fung. Compressibility and constitutive equation of arterial wall in radial compression experiments. *J Biomech*, 17:35–40, 1984.

[12] C. J. Chuong and Y. C. Fung. Residual stress in arteries. In G. W. Schmid-Schobein, S. L. Y. Woo, and B. W. Zweifach, editors, *Frontiers in Biomechanics*, chapter 9, pages 117–129. Springer-Verlag, New York, 1986.

[13] J. M. Clark and S. Glagov. Transmural organization of the arterial media. *Arteriosclerosis*, 5(1):19–34, 1985.

[14] P. F. Davies. Flow-mediated endothelial mechanotransduction. *Math Phys*, 75:519–560, 1995.

[15] M. Destrade, G. Saccomandi, and I. Sgura. Inhomogeneous shear of orthotropic incompressible non-linearly elastic solids: Singular solutions and biomechanical interpretation. *Int J Eng Sci*, 47:1170–1181, 2009.

[16] J. F. Eberth, L. Cardamone, and J. D. Humphrey. Evolving biaxial mechanical properties of mouse carotid arteries in hypertension. *J Biomech*, 44:2532–2537, 2011.

[17] J. F. Eberth, V. C. Greshamb, A. K. Reddyc, N. Popovicd, E. Wilsond, and J. D. Humphreya. Importance of pulsatility in hypertensive carotid artery growth and remodeling. *J Hypertension*, 27(10):2010–2021, 2009.

[18] A. E. Ehret and M. Itskov. A polyconvex hyperelastic model for fiber-reinforced materials in application to soft tissues. *J Mater Sci*, 42:8853–8863, 2007.

[19] M. Epstein and A. Goriely. Self-diffusion in remodeling and growth. *Z Angew Math Phys*, 63:339–355, 2012.

[20] P. Fridez, A. Rachev, J. J. Meister, K. Hayashi, and N. Stergiopulos. Model of geometrical and smooth muscle adaptation of carotid artery subject to step change in pressure. *Am J Physiol Heart Circ Physiol*, 280:H2752–2760, 2001.

[21] Y. C. Fung. *Biomechanics: Motion, Flow, Stress, and Growth*. Springer-Verlag, New York, 1990.

[22] Y. C. Fung. *Biomechanics. Mechanical Properties of Living Tissues*. Springer-Verlag, New York, 2nd edition, 1993.

[23] Y. C. Fung. Stress, strain, growth, and remodeling of living organisms. *Z Angew Math Phys*, 46:S469–S482, 1995.

[24] Y. C. Fung and S. Q. Liu. Changes of zero-stress state of rat pulmonary arteries in hypoxic hypertension. *J Appl Physiol*, 70:2455–2470, 1991.

[25] K. Garikipati, E. M. Arruda, K. Grosh, H. Narayanan, and S. Calve. A continuum treatment of growth in biological tissue: the coupling of mass transport and mechanics. *J Mech Phys Solids.*, 52:1595–1625, 2004.

[26] T. C. Gasser, R. W. Ogden, and G. A. Holzapfel. Hyperelastic modeling of arterial layers with distributed collagen fibre orientation. *J R Soc*, 3:15–35, 2006.

[27] G. H. Gibbons and V. J. Dzau. The emerging concept of vascular remodeling. *N Eng J Med*, 330:1431–1438, 1994.

[28] Y. Gorb and J. R. Walton. Dependence of the frequency spectrum of small amplitude vibrations superimposed on finite deformations of a nonlinear, cylindrical elastic body on residual stress. *Int J Eng Sci*, 48(11):1293–1312, 2010.

[29] A. Goriely and M. Ben A. On the definition and modeling of incremental, cumulative, and continuous growth laws in morphoelasticity. *Biomech Model Mechanobiol*, 6:289–296, 2007.

[30] K. Gou and J. R. Walton. Reconstruction of nonuniform residual stress for soft hyperelastic tissue via inverse spectral techniques. *Int J Eng Sci*, 82:46–73, 2014.

[31] F. Grinnell. Fibroblast biology in three-dimensional collagen matrices. *Trends Cell Biol*, 13:264–269, 2003.

[32] F. Guilak, D. L. Butler, S. A. Goldstein, and F. P. T. Baaijens. Biomechanics and mechanobiology in functional tissue engineering. *J Biomech.*, 47:1933–1940, 2014.

[33] A. Guillou and R. W. Ogden. Growth in soft biological tissue and residual stress development. In G. A. Holzapfel and R. W. Ogden, editors, *Mechanics of Biological Tissue*. Free Press, 2006.

[34] G. A. Holzapfel, T. C. Gasser, and R. W. Ogden. A new constitutive framework for arterial wall mechanics and a comparative study of material models. *J Elasticity*, 61:1–48, 2000.

[35] J. D. Humphrey. *Cardiovascular Solid Mechanics*. Springer-Verlag, New York, 1st edition, 2002.

[36] J. D. Humphrey. Vascular adaptation and mechanical homeostasis at tissue, cellular, and sub-cellular levels. *Cell Biochem Biophys*, 50:53–78, 2008.

[37] J. D. Humphrey. Vascular mechanics, mechanobiology and remodeling. *J Mech Med Biol*, 9(2):243–257, 2009.

[38] J. D. Humphrey, J. F. Eberth, W. W. Dyea, and R. L. Gleason. Fundamental role of axial stress in compensatory adaptations by arteries. *J Biomech.*, 42:1–8, 2009.

[39] J. D. Humphrey and G. A. Holzapfel. Mechanics, mechanobiology, and modeling of human abdominal aorta and aneurysms. *J Biomech.*, 45:805–814, 2012.

[40] J. D. Humphrey and K. R. Rajagopal. A constrained mixture model for growth and remodeling of soft tissues. *Math Model Meth Appl Sci*, 12(3):407–430, 2002.

[41] J. D. Humphrey and K. R. Rajagopal. A constrained mixture model for arterial adaptations to a sustained step change in blood flow. *Biomech Model Mechanobiol*, 2:109–126, 2003.

[42] S. Joshi and J. R. Walton. Reconstruction of the residual stresses in a hyperelastic body using ultrasound techniques. *Int J Eng Sci*, 70:46–73, 2013.

[43] E. Kuhl, R. Maas, G. Himpel, and A. Menzel. Computational modeling of arterial wall growth. *Biomech Model Mechanobiol*, 6:321–331, 2007.

[44] B. L. Langille. Remodeling of developing and mature arteries: endothelium, smooth muscle, and matrix. *J Cardio Pharm*, 21:S11–S17, 1993.

[45] S. Lehoux, Y. Castier, and A. Tedgui. Molecular mechanisms of the vascular responses to haemodynamic forces. *J Intern Med*, 259:381–392, 2006.

[46] D. Y. M. Leung, S. Glagov, and M. B. Mathews. Cyclic stretching stimulates synthesis of matrix components by arterial smooth muscle cells in vitro. *Sci*, 191(4226):475–477, 1976.

[47] C. Li and Q. Xu. Mechanical stress-initiated signal transduction in vascular smooth muscle cells in vitro and in vivo. *Cell Signal*, 19:881–891, 2007.

[48] S. Q. Liu and Y. C. Fung. Zero-stress state of arteries. *J Biomech Eng*, 110:82–84, 1988.

[49] S. Q. Liu and Y. C. Fung. Relationship between hypertension, hypertrophy, and opening angle of zero-state of arteries following aortic constriction. *J Biomech Eng*, 111:325–335, 1989.

[50] A. Lubarda and A. Hoger. On the mechanics of solids with a growing mass. *Int J Solids Struct*, 39:4627–4664, 2002.

[51] I. Masson, H. Beaussier, P. Boutouyrie, S. Laurent, J. D. Humphrey, and M. Zidi. Carotid artery mechanical properties and stresses quantified using in vivo data from normotensive and hypertensive humans. *Biomech Model Mechanobiol*, 10:867–882, 2011.

[52] T. Matsumoto and K. Hayashi. Stress and strain distribution in hypertensive and normotensive rat aorta considering residual strain. *J Biomech Eng*, 118:62–73, 1996.

[53] W. R. Milnor. Principles of hemodynamics. In W. R. Milnor, editor, *Cardiovascular Physiology*. Oxford University Press, 1990.

[54] G. Olivetti, P. Anversa, M. Melissari, and A. V. Loud. Morphometry of the renal corpuscle during postnatal growth and compensatory hypertrophy. *Kidney International*, 17:438–454, 1980.

[55] L. Olsen, J. A. Sherratt, P. K. Maini, and F. Arnold. A mathematical model for the capillary endothelial cell-extracellular matrix interactions in would-healing angiogenesis. *IMA J Math Appl Med Biol*, 14:261–281, 1997.

[56] G. K. Owens. Control of hypertrophic versus hyperplastic growth of vascular smooth muscle cells. *Am J Physiol*, 257:H1755–H1765, 1989.

[57] G. K. Owens and M. A. Reidy. Hyperplastic growth response of vascular smooth muscle cells following induction of acute hypertension in rats by aortic coarctation. *Circ Res*, 57:697–705, 1985.

[58] A. Rachev, N. Stergiopulos, and J. J. Meister. A model for geometric and mechanical adaptation of arteries to sustained hypertension. *J Biomech Eng*, 120:9–17, 1998.

[59] A. Rachev, W. R. Taylor, and R. P. Vito. Calculation of the outcomes of remodeling of arteries subjected to sustained hypertension using a 3d two-layered model. *Annals Biomed Eng*, 41(7):1539–1553, 2014.

[60] M. K. Rausch, A. Dam, S. Gktepe, O. J. Abilez, and E. Kuhl. Computational modeling of growth: systemic and pulmonary hypertension in the heart. *Biomech Model Mechanobiol*, 10:799–811, 2011.

[61] J. A. G. Rhodin. Architecture of the vessel wall. In R. M. Berne, editor, *Handbook of Physiology*. American Physiological Society, 1979.

[62] E. K. Rodriguez, A. Hoger, and A. D. Mcculloch. Stress-dependent finite growth in soft elastic tissues. *J Biomech*, 27(4):455–467, 1994.

[63] L. H. Romer, K. G. Birukov, and J. G. N. Garcia. Focal adhesions paradigm for a signaling nexus. *Circ Res*, 98:606–616, 2006.

[64] L. A. Rosen, T. H. Hollis, and M. G. Sharma. Alterations in bovine endothelial histidine decarboxylase activity following exposure to shear stress. *Exp Mol Pathol*, 20:329–343, 1974.

[65] R. Skalak. Growth as a finite displacement field. In D.E Carlson and R.T. Shield, editors, *Proc. IUTAM Symposium on Finite Elasticity*. Martinus Nijhoff, 1981.

[66] R. Skalak, G. Dasgupta, M. Moss, E. Otten, P. Dullemeijer, and H. Vilmann. Analytic discription of growth. *J theor Biol*, 94:555–577, 1982.

[67] P. Sez, E. Pea, M. A. Martnez, and E. Kuhl. Computational modeling of hypertensive growth in the human carotid artery. *Comput Mech*, 53:1183–1196, 2014.

[68] L. A. Taber. Biomechanics of growth, remodeling and morphogenesis. *Appl Mech Rev*, 48(8):487–543, 1995.

[69] L. A. Taber. A model for aortic growth based on fluid shear and fiber stresses. *J Biomech Eng*, 120:348–354, 1998.

[70] L. A. Taber and D. W. Eggers. Theoretical study of stress-modulated growth in the aorta. *J Theor Biol*, 180:343–357, 1996.

[71] L. A. Taber and J. D. Humphrey. Stress-modulated growth, residual stress, and vascular heterogeneity. *J Biomech Eng*, 123:528–535, 2001.

[72] A. Valentn, L. Cardamone, S. Baek, and J. D. Humphrey. Complementary vasoactivity and matrix remodelling in arterial adaptations to altered flow and pressure. *J R Soc*, 6:293–306, 2009.

[73] A. Valentn and J. D. Humphrey. Modeling effects of axial extension on arterial growth and remodeling. *Med Biol Eng Comput*, 47:979–987, 2009.

[74] B. Williams. Mechanical influences on vascular smooth muscle cell function. *J Hypertension*, 16:1921–1929, 1998.

[75] H. Wolinsky. Comparison of medial growth of human thoracic and abdominal aortas. *Circ Res*, 27:531–538, 1970.